KENYATTA UNIVERSITY

SOLAR STILL BASIN MEASUREMENTS AND LINER MATERIAL VARIANCE FOR IMPROVED WATER DESALINATION EFFICIENCY

RUTH NJOKI NJUGUNA
(BSC. ELECTRICAL AND ELECTRONIC ENGINEERING)
J104/CTY/PT/39097/2017
DEPARTMENT ENERGY, GAS & PETROLEUM ENGINEERING

A THESIS SUBMITTED IN PARTIAL FULFILMENT OF THE REQUIREMENTS FOR THE AWARD OF THE DEGREE OF MASTER OF SCIENCE IN RENEWABLE ENERGY TECHNOLOGY IN THE SCHOOL OF ENGINEERING AND ARCHITECTURE OF KENYATTA UNIVERSITY

2025

Declaration

Student

This thesis is my original work and has not been presented for a degree award in this or any other university.

Sign..... Date.....

Ruth Njoki Njuguna

J104/CTY/PT/39097/2017

Supervisors

This thesis has been submitted with our approval as supervisors:

Sign..... Date.....

Dr. Francis Njoka

Department of Energy, Gas and Petroleum Engineering, Kenyatta University

Sign..... Date.....

Dr. Joseph Muguthu

Department of Energy, Gas and Petroleum Engineering, Kenyatta University

Dedication

This thesis is dedicated to my family, whose steadfast support and encouragement have been the cornerstone of my journey. Their confidence in my capabilities has motivated me to pursue excellence and overcome obstacles. I also extend this dedication to the trailblazers of solar energy research, whose invaluable contributions have provided the foundation for this study.

Acknowledgements

First and foremost, I am deeply grateful to the Gracious God for His unwavering faithfulness. I extend my heartfelt appreciation to my supervisors, Dr. Francis Njoka and Dr. Joseph Muguthu, for their exceptional guidance, insightful feedback, thoughtful comments, patience, and unwavering encouragement throughout this journey. I am especially thankful to my colleagues and friends for their continual support and motivation. My deepest gratitude goes to my family for their unwavering encouragement and understanding in the course of this research. Lastly, I sincerely thank everyone who contributed in any way to the successful completion of this work.

Table of Contents

List of Tables

List of Figures

List of Abbreviations and Acronyms

ANSYS	Analysis System
CFD	Computational Fluid Dynamics
COMSOL	Computer and Solution
GNU	Gnu's Not Unix
MATLAB	Matrix Laboratory
PCM	Phase Change Material
SciLAB	Scientific Laboratory
SDG	Sustainable Development Goals
TDS	Total Dissolved Salts
TRNSYS	Transient System Simulation
USGS	United States Geological Survey
WHO	World Health Organization

Nomenclature and Symbols

A_g – Glass cover area in m^2

A_w – Water area in m^2

A_b – Basin area in m^2

α_g – Glass cover absorptivity

α_g – water absorptivity

α_b – liner material absorptivity

BW - Back wall height in m

C_{brine}= salt fraction

Cg - specific heat of glass in J/kg.K

C_w - specific heat of water in J/kg.K

C_b - specific heat of liber material in J/kg.K

Δm_d= daily distillate mass

Δt - Time interval

d- Liner material thickness

ρ – Density

ε_{eff} - Effective Emissivity

ε_w - water Emissivity

ε_g – glass cover Emissivity

f_e - entrainment fraction

FW - Front wall height.

GCIA - Glass cover material inclination angle

h_{cga} - convective heat transfer coefficient between the glass cover and air in W/m^2K

h_{rga} - radiative heat transfer coefficient between the transparent and air in W/m^2K

h_{cwg} - convective heat transfer coefficient between the water and glass cover in W/m^2K

q_{conbw} - Conductive heat transfer from the basin liner to the water

h_{rba} - radiative heat transfer coefficient between the basin and air in W/m^2K

I_T - Incident solar radiation in W/m^2

k - thermal conductivity of the basin liner material W/mK

L – Basin Length

L_w - Latent heat of vaporization

m_b – mass of basin

m_{ew} – Freshwater production rate

m_g – mass of gloss cover

m_w – mass of water

η – Solar still efficiency

P_g - glass surface partial vapour pressure

P_w – water surface partial vapour pressure

q_{cga} – Convective heat transfer from the transparent cover to air

q_{rga} - Radiative heat transfer from the transparent cover to air

q_{ewg} - Evaporative heat transfer from the water to the glass

q_{rwg} - Radiative heat transfer from the water to the glass

q_{cwg} - Convective heat transfer from the water to the glass

q_{cba} - Convective heat transfer from the basin liner to surrounding air.

h_{rwg} - radiative heat transfer coefficient between the water and glass cover in W/m^2K

h_{ewg} - evaporative heat transfer coefficient between the water and glass cover in W/m^2K

h_{conbw} - conductive heat transfer coefficient between the basin and water in W/m^2K

h_{cbw} - convective heat transfer coefficient between the basin and water in W/m^2K

h_{cba} - convective heat transfer coefficient between the basin and air in W/m^2K

q_{cbw} - Convective heat transfer from the basin liner to the water

TDS – Total Dissolved Solids

$m_{salt,d}$ – Mass of Dissolved Salts

V_d – Distillate Volume

q_{rba} - Radiative heat transfer from the basin liner to surrounding air.

Q_{abs} – Energy absorbed by the basin liner

R_{th} – Thermal resistance

SSBL – Solar Still basin length

$\boldsymbol{\sigma}$ - Stephan-Boltzmann constant value 5.67 $\times 10^{-8}$ $W/m^2. K^4$

T_a - Surrounding air Temperature.

T_b - Basin liner temperature.

T_g – Glass cover temperature

T_w – Water temperature.

τ_g - Glass cover transmissivity

τ_w - water transmissivity

W – Basin Width

Abstract

Access to potable water is a persistent global challenge. To address this, clean drinking water can be obtained from the abundant saline sources through solar desalination. Solar stills offer a sustainable and environmentally friendly solution; however, their desalination efficiencies remain relatively low. The impact of basin width to length ration measurements and liner material variance on their performance have not been adequately evaluated. This study aimed to model the thermal performance of a single-slope solar still, assess the influence of basin liner materials and their thicknesses on desalination efficiency, and determine the optimal basin dimensions for improved freshwater production. This was done with the objective of improving the performance of a one-slope solar desalination still. MATLAB is employed in the model development and simulations. The developed model was validated using experimental data from literature. The analysis used Machakos Kenya (1.52 °S, 37.2 °E) climatic conditions as a reference. Five basin liner materials including aluminium, synthetic graphite, brass, galvanized iron and stainless steel were examined based on their thermal properties. Different width-to-length ratios ranging from 0.14 to 0.86 and basin liner thicknesses of between 2 mm and 6 mm were evaluated. A parametric study was conducted to determine the correlation between liner material thickness and basin dimensions, and their combined impact on freshwater yields. From the results, synthetic graphite exhibited the best performance, followed by aluminium, brass, galvanized iron and stainless steel with respective yields of 3835g/m^2.day, 2626 g/m^2.day, 1864 g/m^2.day, 1545 g/m^2.day and 1354 g/m^2.day corresponding to efficiencies of 35.04%, 24.02%, 17.02%, 14.13% and 12.39%, respectively. Thus, synthetic graphite outperformed aluminium, brass, galvanized iron and stainless steel by 31.4%, 51.43%, 59.675 and 64.64%, respectively. A width-to-length ratio of 0.45 yields optimal results, while a liner material thickness of 4 mm is found to be ideal across all materials. The parametric study further revealed that width-to-length ratio has a higher significance on freshwater yields compared to liner material thickness.

CHAPTER ONE

INTRODUCTION

1.1 Background

Water scantiness is an increasingly pressing global challenge affecting a myriad of humans and ecosystems. For human life, water is a basic need for survival. Availability of clean consumption water is part of the main dimensions of human well-being as it contributes to good health, (World Bank, 2020). As population growth, industrialization and climate change intensify, the demand for freshwater outpaces the available supply. Based on the United Nations Report (2021), an estimated 2 billion humans live in areas that encounters strain with acquisition to safe drinking water while at least 4 billion others experience water scarcity at least 30 days in a year. The rising global demand for water resources contributes to the increasing depletion of freshwater reservoirs as expressed by Kabeel et al. (2024). Availability of potable water for consumption is among the fundamental dimensions of human well-being as it contributes to good health, (World Bank, 2020).

The distribution of this valuable resource is also uneven, with the giant share falling under salty water (Hassan et al., 2022). This coupled with population growth, environmental pollution, urbanization, industrialization and climate change further exacerbates the freshwater scarcity situation as highlighted by Suraparaju et al. (2024). The situation is worst in the developing world. The challenge of freshwater scarcity is even more pronounced in Kenya, where the country is classified as water-scarce, with renewable freshwater availability estimated at less than 600 m^3 per person per year, far below the global benchmark of 1,000 m^3 per person per year that defines water scarcity (World Bank, 2021), (FAO, 2020). Rapid population growth, erratic rainfall, and climate change have further exacerbated the situation, particularly in regions such as Machakos, where communities often rely on saline or brackish groundwater sources (The National Water Resources Strategy, 2021).

To improve the situation, many scientists continue to explore and come up with innovative solutions to address the increasing demand for potable water (Singh, 2023). Some of these methods involve purification/desalination of the abundant salty water to obtain potable water. Some of the desalination processes utilize fossil fuels to power the process thus unsustainable and polluting while others utilize renewable sources of energy including solar (Rejeb et al., 2021).

One of the most simple and inexpensive technological innovations is the solar still (Ayoobi & Ramezanizadeh, 2022). This is a saline water desalination device that uses the free, green energy from the sun, hence falling in the realm of sustainable development (Kumar & Maurya, 2022). Solar distillation systems should be economic, self-sustainable and environment-friendly (Singh & Samsher, 2021). Because of its simple construct, it is easy to operate and maintain therefore very suitable, especially for the low-income earners in the developing world (Santos & Hernandez, 2017). The elementary design of a solar still entails a one-basin with a single or dual-slope, which is made of materials of low specific heat capacity to reduce the portion of heat required for temperature rise and high thermal conductivity for faster energy flow. Despite the many advantages of the one slope passive solar still, the system's major shortcoming is low efficiency (Hafs et al., 2023). Due to this challenge, several scientists have in the recent decades conducted several studies using both experiments and simulations in an endeavour to come up with a more efficient passive solar still.

Most of these studies have involved structure enhancement to improve the amount of the produced distillate. Various aspects impact the output of the one-slope solar desalination still. Solar insolation for instance, being the amount of solar insolation received, directly impacts its productivity. Higher solar insolation leads to greater energy input for evaporation, which in turn results in increased freshwater production. The Ambient temperature also has a proportionate relationship with evaporation. The design, basin measurements, cover material inclination, liner material, depth of brackish water and insulation all play vital roles in heat absorption and retention, affecting the overall efficiency of the system.

1.2 Problem Statement

Freshwater scarcity is a pressing global issue, whereas salty water remains abundant (United Nations Water., 2021). In response to the escalating demand for freshwater, salty water desalination techniques have been developed over time. Among the emerging methods, solar desalination has shown promising potential as the utilized energy source is free, green and sustainable in nature (Qasim et al., 2019). According to El-Sebaii & El-Bialy (2015), one of the simplest, cost-effective designs of solar desalination techniques which can be accessed by low-income earners in the developing world is the simple one-slope solar desalination still. However, the efficiency of this solar still type remains low. The efficiency of solar stills is largely influenced

by solar insolation, ambient temperature, basin width-to-length measurements, transparent cover material inclination, liner material and thickness, water depth among others (Omara et al., 2014). Solar still basin measurements play a critical function in solar desalination stills productivity as they influence the solar radiation exposure hence the evaporation rate (Tiwari & Sahota, 2017). Similarly, the liner material is a vital component of the solar desalination still, as it governs how effectively the absorbed solar energy is transferred to the saline water, thereby increasing evaporation (Thakur et al., 2022). Despite the importance of these parameters, the extent to which the solar still width-to-length measurements and basin liner material variance affect the performance of a simple one-slope solar desalination still has not been sufficiently evaluated, particularly under Kenyan climatic conditions.

1.3 Justification of Research

Freshwater scarcity continues to pose a major global and national challenge, particularly in arid and semi-arid regions where groundwater and surface water resources are either depleted or saline. Kenya, like many developing countries, faces acute water shortages that threaten both domestic supply and sustainable development. Conversely, saline and brackish water sources are abundant and, when coupled with the freely available solar energy, present a viable alternative for freshwater production through solar desalination.

Researchers such as (El-Sebaii et al., 2015) and (Feilizadeh et al., 2017) have emphasized the need to improve the thermal performance of simple solar stills by optimizing design parameters. However, despite extensive studies, there remains a shortcoming in understanding the combined influence of basin liner material, thickness, and basin geometry on overall still efficiency. This study, therefore, responds directly to those identified research gaps by systematically investigating how basin liner characteristics and basin aspect ratio affect productivity and efficiency under realistic solar conditions. The investigation is driven by the conviction that an optimized single-slope solar still, constructed using locally available materials, can significantly enhance freshwater output and lower the cost of sustainable water production. Beyond the technical contribution, the outcomes of this study hold strong societal relevance. The findings can guide efforts towards low-cost desalination solutions aligned with (SDG 6, 2015) (Clean Water and Sanitation). Thus, this research not only bridges a scientific gap but also contributes directly to environmental sustainability and the socio-economic well-being of water-scarce communities.

1.4 Research Objectives

1.4.1 General Objective

To analyze how geometric configuration and basin liner material characteristics influence the performance of a single slope solar still.

1.4.2 Specific Objectives

1. To model the performance of solar still under different basin width-to length dimensions.
2. To simulate the performance of solar still under different basin liner material types and thicknesses.
3. To conduct a parametric study of the solar still based on basin dimensions and selected liner material thickness.

1.5 Research Questions

The research questions are outlined as follows:

1. How does the liner material influence heat and mass transfer behaviour in a solar desalination still and does its selection influence the solar still's performance?

2. How do variations in the basin liner material thickness and solar still basin dimensions affect the freshwater yield and efficiency of a solar still and if so by what extent?

3. What is the correlation between basin dimensions and liner material thickness?

1.6 Study Significance

Water scarcity is one of the main challenges faced in many regions worldwide. With the world's inhabitants constantly increasing, the freshwater demand also increases. Water scarcity is predicted to worsen in the future. Improving water desalination efficiency can provide a reliable source of freshwater for people living in areas with water scarcity. Use of clean green energy in the form of solar energy to power water desalination is an environmentally friendly and sustainable approach. By improving the design of solar stills, researchers can increase the efficiency of the desalination equipment and reduce the price of producing fresh water. Researching the solar still basin dimensions and basin liner material for improved water desalination efficiency can contribute to scientific advancements in the field of renewable energy and sustainable development. This can lead to the discovery of new materials and technologies that can be used to amplify the efficiency of solar desalination stills and other renewable energy systems.

1.7 Study Scope

This study entailed mathematical modelling to simulate the behaviour of a one-slope solar still under various dimensions and liner materials and thicknesses. Different dimensions and material thicknesses were defined guided by literature. The equations for various modes of heat transfer including convection, radiation, conduction and vaporization were included. The mass flow within the solar still was also evaluated. Machakos (1.52 °S, 37.2 °E), Kenya climatic conditions were considered for the design because of its high irradiation (Kenya Meteorological Department) and abundant saline underground water. The study was limited to modelling, simulations and comparisons with existing experimental results in literature. Besides the basin dimensions and liner materials and thicknesses, other still parameters were not part of the study.

1.8 Study Limitations

During the study, some limitations that could affect the generalization of the findings were identified. For instance, climatic analysis for Machakos was limited to two representative cases per month rather than covering the entire year. The study also does not account for the long-term durability or maintenance requirements of the selected basin liner materials, which could influence their practical application. Time constraints were also encountered in the study execution. Various assumptions that were made during model development could also bring forth slight variations between the model work and physical implementations.

1.9 Conceptual Framework

This study is conceptually grounded on the thermal performance relationship between solar still design parameters and freshwater production. The independent variables are basin liner material type, liner thickness and basin dimensions (expressed as width-to-length ratio). These parameters govern the basin liner's thermal conductivity, heat retention capacity, and internal thermal resistance, which together determine the rates of conduction and convection into the water. The dependent variables are glass, water and basin temperatures, freshwater yield and solar still efficiency, the primary performance metrics of the solar still. Extraneous variables such as solar irradiance, ambient temperature and wind speed influence performance but are treated as external inputs in the model rather than controlled experimental variables. The framework therefore posits that liner material and thickness, combined with basin geometry, drive internal heat transfer and evaporation processes, and thus determine freshwater output under given climatic conditions.

CHAPTER TWO

LITERATURE REVIEW

2.1 Introduction

This chapter reviews the existing literature on solar desalination technology, focusing on solar stills. It addresses the current state of potable water access, methods for desalinating saline water, and the various categories of solar stills. The working principle of a single-slope solar desalination still is discussed, along with the factors influencing its performance. Additionally, the modeling of solar stills is explored, and key equations governing their operation are presented. The chapter concludes with a summary of related studies and identifies the gaps in existing research.

2.2 Theoretical Background

2.2.1 Access to Potable Drinking Water

Water is a fundamental component of all life. It is the main constituent of animal and plant cells, without which there can be no life. Not only is it required to sustain life but for numerous other processes including cooking, cleaning, transportation, cooling, manufacturing construction, recreation, power generation among many others. Even though water is essential for all the above and other processes, it is unfortunately not so readily available, and its distribution is very uneven, with 97% being saline and barely 3% being fresh water, (USGS Report, 2018). Out of the 3% fresh water, only approximately 30% of it can be easily accessed as the larger amount of it is trapped in ice and glaciers (USGS Report, 2021). The situation is further exacerbated by the rapid population growth worldwide, making it unavailable for all, especially in the developing countries. Global warming and climate change do not make the situation any better. The rise in temperature causes the melting of glaciers and ice and the trapped freshwater adds to the oceans and seas, further reducing the percentage of freshwater (Al-Maliki et al., 2022). Rise in temperature further causes uneven distribution of precipitation, causing floods in some areas and drought in others. Floods can lead to contamination of the available water, (Mandal et al., 2021). This elucidates that fresh water is indeed a very scarce resource, and measures must be taken to ensure that more people get access to it. The challenge of freshwater scarcity is even more pronounced in Kenya, where the country is classified as water-scarce, with renewable freshwater availability estimated at less than 600 m^3 per person per year, far below the global benchmark of 1,000 m^3 per person per year that

defines water scarcity (World Bank, 2021), (FAO, 2020). Rapid population growth, erratic rainfall, and climate change have further exacerbated the situation, particularly in regions such as Machakos, where communities often rely on saline or brackish groundwater sources (The National Water Resources Strategy, 2021). Thus, the need for affordable and sustainable freshwater production solutions is increasingly critical in the Kenyan context. Access to the freshwater resource has major benefits including reduced child mortality, improved hygiene, improved sanitation, economic benefit, reduced disease occurrence, and generally better quality of life. Therefore, it is paramount to improve the availability of the freshwater resource of good quality which complies with SDG 6, (2015), which aims at ensuring sustainable availability of water and sanitation for all.

2.2.2 Water Desalination

One of the ways of improving freshwater access and availability is by purifying the abundant saline water in oceans and boreholes. This can be achieved via various water desalination techniques, which remove salts from the water resulting in clean safe water for consumption. Thus, with the intention of improving freshwater access and availability, various scientists have developed simple inexpensive technological innovations for recovering fresh water from saline water which are known as desalination technics. This is prudent because it is evident that saline water is more readily available, for instance sea and borehole water. Several desalination techniques have been employed over the decades which include reverse osmosis, (Voutchkov, 2017) multi-effect distillation (Cunha et al., 2019) multi-step flash distillation (Mustafa & Al Ghamdi, 2018) among other methods. The above methods however have the limitation that they require to be powered mainly by fossil fuel sources. Fossil fuels are not green sources of energy, in addition to their huge carbon footprint and finite nature, they not only go against sustainable development, but are also costly. This means that most people from the developing world may not be able to have access to them, especially on the small scale. To curb the above limitations, scientists have developed saline water desalination techniques that utilize the clean freely occurring energy from the sun, an example being the solar water purification still.

Solar stills are brackish water desalination equipment that utilize the free, green energy from the sun, making them fall in the realm of sustainable development. Solar desalination stills are easy to manufacture and the cost of their producing it is low while their operation is also not complicated.

Solar stills are also simple and reliable especially in areas that experience high insolation. The water produced by solar stills is clean for human consumption, (Santos & Hernandez, 2017). The elementary design of a solar still entails a one-basin with a single or dual slope, having walls made of materials of low specific heat capacity to reduce the magnitude of heat required for temperature rise and high thermal conductivity for faster energy flow. Solar stills may also be painted black to augment the absorption of the incident solar irradiation. The upper section entails a slanted high transmissivity transparent cover at an angle to allow highest radiation to reach the inside of the solar still. The solar still is properly insulated to minimize the loss of heat to the environment. Salty water is contained inside the basin. Figure 2.1 shows the image of a simple one-slope solar distillation still.

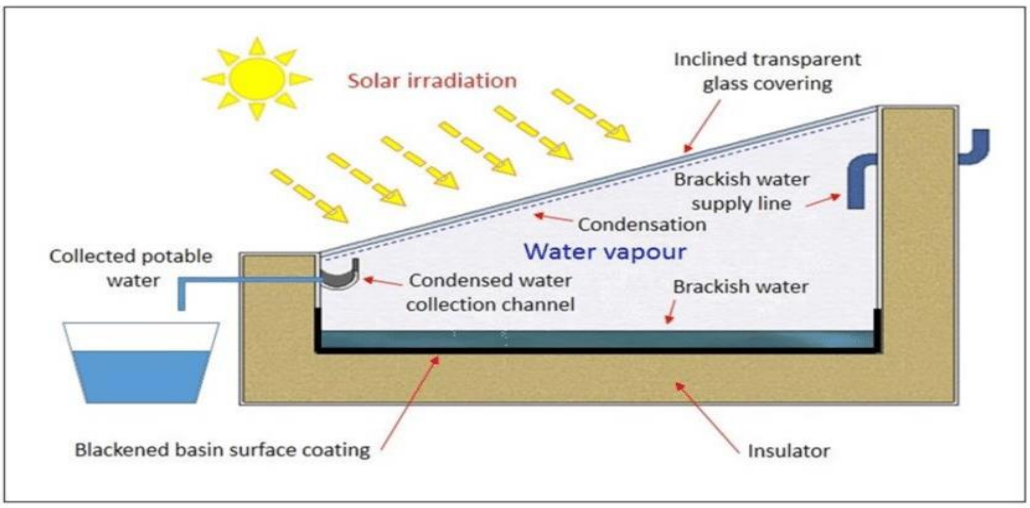

Figure 2.1 One-slope passive solar still (Chamsa-ard et al., 2020)

2.2.3 Solar Still Categories

Solar distillation stills exist in two broad categories, passive and active, (Hemmat Esfe et al., 2021). Passive solar stills utilize the natural sun as their sole source of heat energy. This type of solar still does not have any moving mechanical elements and therefore do not consume power. The principle of operation of a solar still is quite straightforward, (Elango et al., 2015). Most of the heat transfer processes occur within the distillation still. Solar radiation via the slanted transparent cover is trapped inside the solar still and reaches the basin and the walls where it is absorbed. This raises the temperature of the basin heating the brackish water inside it. Evaporation occurs due to the raised water temperature, brackish water-vapour pressure gradient facilitates the evaporation.

Through natural convection, the less dense wet hot air rises reaching the transparent cover. Condensation into liquid water droplets occurs when the wet air is saturated after reaching the transparent cover which is at a lower temperature. These water droplets form the distillate which assemble at the bottom of the transparent cover. This distillate is the purified clean and freshwater that can be used for consumption and for any other freshwater functions, (Mohsenzadeh et al., 2022).

Passive solar stills are typically simpler in design and less expensive to construct and operate. In addition to utilizing the sun's energy, the active category of solar stills contain moving mechanical elements like pumps and valves. Active solar stills may also utilize extra thermal energy from a different source. This is done to enhance the heat generation process. Active solar stills are more expensive and complex than passive solar stills, but they can be more reliable and effective in a wider range of conditions. Several designs of the above desalination still types have been established by scientists over the years and they include one-slope still, double slope still, double basin solar still, pyramid solar still, hemispherical solar still, inverted absorber solar distillation still, tubular distillation still, parabolic distillation still, solar desalination still with phase change materials, desalination still with nano-composite materials, solar still with concentrator among many others (Amir Khadim et al., 2020). Ultimately, the choice of solar distillation still type and design will depend on factors such as the available resources, water purification needs, and environmental conditions in a particular location.

The passive one-slope one-basin solar still has remained attractive especially for portable and domestic applications owing to their simple design and fabrication, small size easing portability, the low cost of fabrication hence allowing access by low income earners, simple operation and maintenance eliminating the need for skilled labour, minimum wear and tear since they have no moving parts and most importantly, they utilize the sun's free, green energy thus convivial to the environment and promotes sustainable development. However, they suffer from the limitation that they depend on the sun, which is not present 24 hours a day and the weather conditions may change to an unfavourable state. Their productivity is also low hence they have low efficiency.

2.2.4 Operation Concept of a One-slope Solar Still.

The elementary design of a solar distillation still entails a unit basin with one-slope, having walls made of materials of minimal specific heat capacity to reduce the amount of heat necessary for

temperature rise and high thermal conductivity for faster energy flow. The upper section features a slanted transparent cover with high transmissivity positioned at an angle to augment the solar irradiation entering the solar desalination equipment. Proper insulation is provided to reduce heat dissipation to the surroundings, and the basin holds the saline water.

The operation of a single-slope solar still is relatively simple (Chamsa-ard et al., 2020) Solar energy passes through the transparent cover, typically made of glass or plastic, and is absorbed by the water surface and other sections of the still, among them the transparent cover, the water, and the basin liner (Lisboa et al., 2022). This absorption raises the temperature of the saline water, causing it to evaporate and leave behind salt and impurities. Vapor rises and condenses on the cooler underside of the transparent cover, forming droplets. These droplets flow down the slanted surface of the cover and are collected in a reservoir at the bottom, where they are stored as fresh water. The residual salt and impurities remain in the basin and require periodic removal to maintain the still's efficiency (Elango et al., 2015).

2.2.5 Aspects Influencing the Performance of a Passive One-slope Solar Desalination Still.

The principal idea to improving a solar still's efficiency is directly dependent on two driving forces, which are high water temperature and low inner cover material temperature, (Panchal & Awasthi, 2017). The former ensures that more water vapourizes while the latter ensures that more vapour is condensed into fresh water. Minimization of heat loss to the environment also plays a key role. The above may be controlled by three major factors, including environmental conditions, design and operating conditions of the desalination still. The environmental conditions affecting the desalination equipment's performance are climatic aspects like solar insolation, wind velocity and ambient temperature (Hemmat Esfe et al., 2021). Among them, the intensity of solar radiation bears the heaviest effect on freshwater productivity (Rejeb et al., 2021).

Design conditions affecting solar still performance are factors involving the physical construct of the solar still and include solar still basin dimensions, glazing cover type and inclination, (Hassan et al., 2022), insulating material and its thickness, liner material and its thickness, evaporative and exposure surface areas among others. Other factors affecting the performance of the water purification equipment are operating conditions which are the conditions when the solar still is in

operation and among them is transparent cover temperature, basin water temperature, basin water depth among others (El-Sebaey et al., 2022).

2.2.6 Modelling Direct Solar Still Systems

Models are feigned worlds built to represent the actual world while experiments are variants of the actual world encapsulated within an artificial laboratory environment. Various aspects in a scientific model can be easily varied to simulate various possible results (Ebaid & Ammari, 2015). Such variations can be hectic when using prototypes which are also expensive and time consuming. As such, models are cheaper, they enable us to test a system before deploying it into the real world, and they can be used to perform predictions and optimizations (Bansal et al., 2022).

From the foregoing, it is observed that most researchers are adopting modelling as a means of coming up with new discoveries. The major types of models usually employed in engineering designs include mathematical models, numerical models and physical models. Mathematical models use equations to describe real life phenomena (Ghanim, 2008). They allow for the design process to be flexible and various output conditions can be achieved by varying the various input parameters (Ayoobi & Ramezanizadeh, 2022). They are useful in solving optimization problems. Numerical models on the other hand refer to mathematical models in cases where the systems are complex. The system is broken down into smaller sections which are solved, and the solutions integrated to represent the whole system. As such, predictions from modelling processes are very beneficial as they provide flexibility in input parameter variations. This provides a great platform for discovery of optimum combinations of those input parameters, and this helps in testing how far the solar still design can be optimized to improve efficiency. Models through simulation consume less time in testing compared to testing fabricated solar stills, (Ayoobi & Ramezanizadeh, 2022).

The basic steps involved in modelling a direct solar still system involve geometry and dimensions of the system definition, including the size and shape of the basin, the thickness and cover material, the material and thickness of the basin liner and other components such as insulation. Thermodynamic properties of the materials used in the system, including the thermal conductivity and specific heat capacity of the cover material, basin liner, the thermal conductivity of the insulation, and the density of the water are then defined. The various boundary conditions for the system, including the solar irradiation intensity, the surrounding temperature and humidity, and

the temperature and humidity of the water surface are also defined, (Malaeb et al., 2016). This leads to the development of mathematical equations that describe the heat and mass transfer activities that take place in the system, including equations for the solar irradiation absorption, the heat transfer through the cover material and water evaporation.

The developed equations are then solved using mathematical or numerical methods to obtain a set of results that describe the temperature profile in the system. The model is then authenticated by comparing the predicted outcomes with similar previous data or using data from experiments. The model is used to optimize the design of the direct solar still system, by varying the system parameters for instance the size of the basin, the thickness and material of the cover, basin liner, and the placement of any additional components, to maximize the rate of freshwater production. Overall, modelling a direct solar still system requires a good understanding of the physical and thermal traits of the materials involved, as well as the heat and mass transfer activities that take place. A well-designed model can be a valuable instrument for optimizing the performance of the system and for predicting its behaviour under different operating conditions, (Bansal et al., 2022). Various software like MATLAB, ANSYS Fluent, SciLAB, GNU Octave, TRNSYS, COMSOL Multiphysics, among others, can be used for the modelling and simulation of the system (Prakash et al., 2022).

2.2.7 Solar Still Governing Equations

The phenomena of transfer of heat and balancing of energy control the governing equations of a one-sloped passive solar still. Temperature gradient is the thermodynamic motive force that enables heat transfer. The desalination technique applies the fundamental concepts of evaporation and condensation, (Dhivagar et al., 2022). The various equations describe the physical processes that take place within the solar still and are used to model its performance. In a solar water purification still, most of the heat transfer processes are involved and they include radiation, evaporation, convection and conduction. Thermal resistance models are used to determine heat transfer and energy balance across the various layers. (Beng Yeo et al., 2014). It involves the energy balance of the still's main components. These include the transparent cover, the bulk brackish water and the basin itself.

The transparent cover obtains heat from the bulk water via convection, evaporation and radiation as well as from the sun. It loses energy to the nearby air mainly via convection and radiation. The

bulk water receives a fragment of the incident radiation past the transparent cover and from the basin via conduction and convection. The basin liner receives a fraction of the incident radiation while losing heat to the bulk water by convection and conduction and to the neighbouring air via convection and radiation, (Duffie & Beckman, 2013) .

The corresponding energy equilibrium equations for the transparent cover, bulk water and the basin are represented by equations (1), (2) and (3), respectively (Karimi Estahbanati et al., 2016) (Nian et al., 2021), (Feilizadeh et al., 2017). The equations are usually very useful for development of models and prototypes.

$$M_g C_g \frac{dT_g}{dt} = \alpha_g A_g I_T + q_{ewg} + q_{C\omega g} + q_{r\omega g} - q_{cga} - q_{rga} \quad (1)$$

$$M_w C_w \frac{dT_w}{dt} = \tau_g \alpha_w A_w I_T + q_{cbw} + q_{conbw} - q_{ewg} - q_{C\omega g} - q_{r\omega g} \quad (2)$$

$$M_b C_b \frac{dT_b}{dt} = \tau_g \tau_w \alpha_b A_b I_T - q_{cbw} - q_{conbw} - q_{Cba} - q_{rba} \quad (3)$$

2.3 Summary of Related Studies

Passive solar stills remain a desirable brackish water desalination technique for their construction simplicity and low cost (Hemmat Esfe et al., 2021). They can also be fabricated from readily available local materials. As such, they can be easily accessible by low-income earners in the developing world. However, their efficiency is relatively low and in the recent decades, many scientists have conducted several research both experimentally and via modelling in an endeavour to come up with a passive solar still that is more efficient. Inside the evaporation chamber, the heat transfer processes are a combination of evaporation, natural convection as well as radiation between the evaporative (water) and condensation (transparent cover) surfaces. For the studies, the various heat transfers are established by determining the various coefficients of heat transfer.

Dunkle's model, (Dunkle, 1961) is one of the most widely applied correlations in the determination of heat transfer coefficients. He did the initial comprehensive research of solar distillation stills modelling and came up with a theoretical overview of roof type solar stills that highlighted the heat and mass transfer relationships. The model is however unable to predict the water production

with harmonious precision, (Tiwari & Sahota, 2017) some critical aspects for instance solar radiation absorption of the walls, walls heat losses are not considered in the initial Dunkle's model Elango et al. (2015) conducted work to investigate the effect of incorporating thermal models of various solar stills and several features and design considerations were made. They concluded that the one-sloped solar remains a favourite due to its straightforwardness and operation.

Thermal heat capacities impact of basin and transparent cover on the performance of the conventional desalination still through simulations was investigated by Sivakumar et al. (2016) and their study indicated that for the model accounting for basin and transparent cover thermal capacities had a 10% higher yield than the model did factor do this consideration. A review of the performance of thermosiphon evacuated tube collector solar desalination units was done by Singh & Samsher (2021), they reported that the thermosiphon evacuated tube collector assisted solar desalination units as an efficient system and is effective for remote areas.

Flat plate reflectors were applied within the inner walls of a one basin solar desalination still by Karimi Estahbanati et al. (2016) and they found out that internal reflectors on a solar purification equipment's walls can enhance the annual freshwater yield by 34%.

The effect of reducing the still's specific height was investigated by Jamil & Akhtar, (2017) They found out that the water yield increases with decreasing specific height. Kabeel et al. (2017) made use of phase-change materials (PCM) below the solar desalination still's basin to store the surplus heat during peak solar radiation hours and transfer it to the brackish water during the night. Further, Dhivagar et al. (2023) evaluated the performance of a solar still using energy storage biomaterials with a porous surface. Their findings revealed that utilizing conch shells both as an energy storage biomaterial and porous medium improved the total productivity of the solar still by 10.8% compared to a elemental designs.

Nguyen (2018), developed a numerical model to evaluate the performance of basin-type solar distillation systems, covering both elemental passive solar stills and active ones with forced circulation and improved heat recovery. The study examined various factors influencing distillate output, including environmental conditions as well as design and operational parameters. Optimization of these factors was shown to enhance distillate yields by 30 to 68% compared to traditional systems. Kalbasi et al. (2018) proposed a mathematical model to study the impact of

separating the condensing surface and the solar energy receiving surface. Their findings indicated that this separation significantly improved freshwater yield, thereby enhancing the overall output of the solar still. One-sloped still Computational Fluid Dynamics (CFD) was used alongside ANSYS Fluent by Mittal (2021) to simulate a system with various user defined functions, using the lower and upper surface temperatures to estimate various distillation outputs for an entire day.

Feilizadeh et al. (2017) investigated the impact of height, length and width of a one-slope still on its distillate production. Their study revealed that extending the side walls minimized the shadow effect, leading to an increase in the still's efficiency. They identified an optimal width-to-length ratio of 0.4 for enhanced performance. Kabeel et al. (2024) conducted an in-depth analysis of conical solar stills, focusing on their design, performance and various factors that can contribute to improved efficiency. Their findings underscored the advantages of conical stills, including higher efficiency, greater productivity, and cost-effectiveness These benefits were attributed to distinctive design elements like conical shapes, reflectors, and the use of phase-change materials, all of which significantly boost the performance of conical solar desalination stills when compared to conventional models.

2.4 Research Gap

The aforementioned works have been in a bid to have a higher solar still desalination efficiency while still maintaining its low cost. From the studies carried out by researchers in this field and to the best of this authors' knowledge, little or no research has concentrated on the effects of the solar still's basin liner material, its thickness alongside basin dimensions variance on the solar still's efficiency, demonstrating an existing gap. The novelty of the current work is therefore in the development of a thermal model that acknowledges the heat transfer impact at the solar basin's liner and investigates how thermal mass changes with the liner material and its thickness and basin dimensions variation. The objective being to investigate how such variations impact the performance of the one-slope solar still.

CHAPTER THREE

METHODOLOGY

3.1 Introduction

This chapter presents research design, study overview, and experimental setup. It details the procedures followed in the study and the criteria for selecting basin liner materials. The development of the mathematical model, along with the assumptions made, is thoroughly explained. Additionally, the validation of the developed model is discussed. The chapter also outlines the model simulations and the process of recording the data generated from these simulations. Furthermore, the materials used in the study are highlighted, and the methods for data processing and analysis are also covered.

3.2 Research Design

The primary guiding idea was to develop a mathematical model that would simulate the desalination process and accurately predict the efficiency based on varying basin dimensions and the liner material. The research required a comprehensive literature review to identify existing models and theories related to water desalination efficiency. Based on this a conceptual model was developed to represent the relevant physical processes. The research was therefore a modelling-based type of research, with validation done using experimental data in literature. Simulations were done using MATLAB (R2022b) and its Simulink application and the results provided the data range that was analysed to draw conclusions about the still's performance as a factor of basin dimensions and liner material.

3.3 Study Description

The effects of solar still basin dimensions and liner material variation were studied using mathematical modelling which uses equations to describe the heat and mass transfer phenomena. The realized model was validated using experimental data in literature after which it was used to study the solar still's performance. Weather data for a hot and a cooler day for Machakos, a town in Kenya, located at latitude 1.52° south of the equator, and longitude 37.2 east of the prime meridian is incorporated in the model. This was informed by the fact that Machakos has adequate and representative solar insolation and many salty water boreholes.

3.4 Study Setup

No physical setup was done in a laboratory. Simulations were done to determine the various outputs. The setup followed the flow diagram in Figure 3.1.

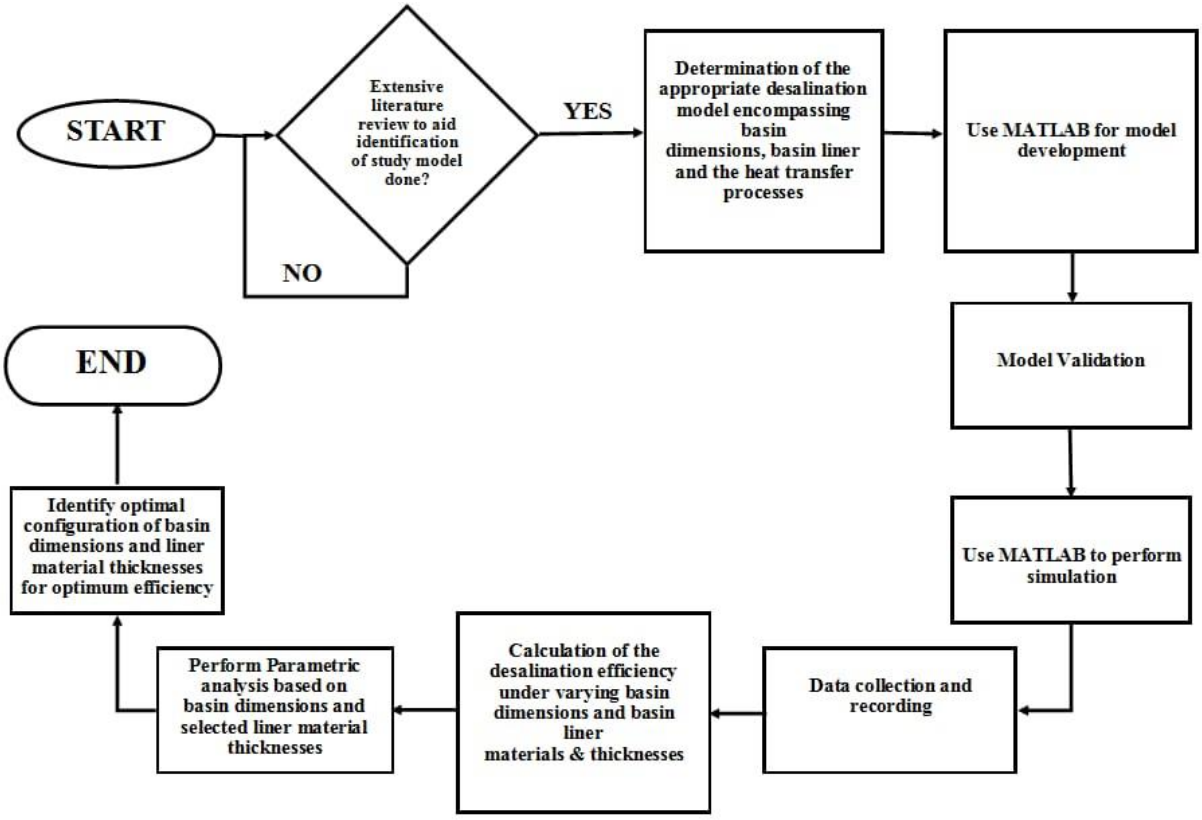

Figure 3.1 Flowchart of the study setup (Source: Author)

3.5 Study Procedures

3.5.1 Parameter Definition

The first step was to define the parameters. The glass-cover thickness was selected to be 4 mm as proposed by Panchal et al. (2021). Since Machakos, with geographic coordinates (1.52 °S, 37.2 °E), is near the equator at a latitude of -1.52°, the optimum glass cover inclination angle would be equivalent to the latitude as stipulated by Suraparaju et al. (2024). The glass cover inclination angle was estimated by subtracting 15° from the latitude of 1.52° to obtain approximately 13.5° as illustrated by G. N. Tiwari & Ahmad (2009). This value provided a slope that ensures freshwater flows into the collection gutter while at the same time the solar still is not too inclined as the location is near the equator for maximum sun radiation contact. The still's fore and rear walls

heights were respectively determined as 0.2 m and 0.44 m. The basin water depth was selected to be 1 cm according to Malik & Mohammad (2023) and Dhivagar et al. (2021), who investigated and found out a lower water depth of 1 cm had a higher freshwater yield. The solar basin area was kept constant at 0.45 m^2. This area was selected as a representative size to ensure manageable computational requirements and realistic scaling to small desalination units. This area provides sufficient surface exposure for reliable modeling of heat and mass transfer processes while maintaining design simplicity and portability. With this constant area, the width-to-length ratios of 0.14, 0.28, 0.45, 0.56 and 0.8 were selected for variation within the model. Subsequently, the resultant mass, volumes and mass-specific heat capacities were calculated. A sawdust insulation of 0.1 m thickness was considered as was investigated by Al-Hinai et al. (2002). Liner material thicknesses of 2 mm, 3 mm, 4 mm, 5 mm and 6 mm were selected for investigation as inputs within the model. The defined width-to-length ratios and liner material thicknesses range were the same values selected for the parametric study.

3.5.2 Liner Material Selection

Solar basin liner materials selected for the study included Aluminium, Brass, Galvanized iron, Stainless Steel and Synthetic Graphite. This was informed by the commonly used still liner materials as well as in exploring the potential of other materials being potent solar still liner materials. The adopted thermal properties of the selected materials like, thermal conductivity and specific heat capacity are defined in Table 3.1.

Table 3.1 Properties of selected materials (Ashby & Jones, 2012, The Engineering Toolbox, Johnson et al., 2019)

Relevant Thermodynamic Parameter	**Numerical Value**
Density of Aluminium	2700 kg/m^3
Density of Brass	8600 kg/m^3
Density of Synthetic graphite	2200 kg/m^3
Density of Galvanized Iron	8600 kg/m^3
Density of Stainless Steel	7800 kg/m^3
Density of Glass	2500 kg/m^3
Density of pure water	1000 kg/m^3
Density of brackish water	1010 kg/m^3
Thermal Conductivity Aluminium	205 W/mK
Thermal Conductivity Brass	109 W/mK
Thermal Conductivity Synthetic Graphite	1500 W/mK
Thermal Conductivity Galvanized Iron	76.2 W/mK
Thermal Conductivity Stainless Steel	50.2 W/mK
Specific Heat Capacity of Aluminium	887 J/kgK
Specific Heat Capacity of Brass	920 J/kgK
Specific Heat Capacity of Synthetic graphite	750 J/kgK
Specific Heat Capacity of Galvanized Iron	462 J/kgK
Specific Heat Capacity of Stainless Steel	468 J/kgK
Specific Heat Capacity of Glass	792 J/kgK
Latent heat of vaporization	2260 J/kg
Emissivity of glass	0.94
Emissivity of water	0.95
Absorptivity of glass	0.05
Absorptivity of water	0.05
Transmissivity of glass	0.86

3.5.3 Mathematical Model Development

A mathematical model to simulate the desalination process and accurately predict the desalination still's performance under varying basin dimensions and liner material was developed. The model represents the relevant physical processes that take place within the solar still. Machakos town (1.52 °S, 37.2 °E), Kenya weather data for the month of March 2024 was used. This data was obtained from the Kenya Meteorological department. From this data, two days were selected and identified as a hotter day (3rd March 2024) and a cooler day (25th March 2024).

Figure 3.2 illustrates the schematic thermal resistance representation of the one-slope solar still under investigation.

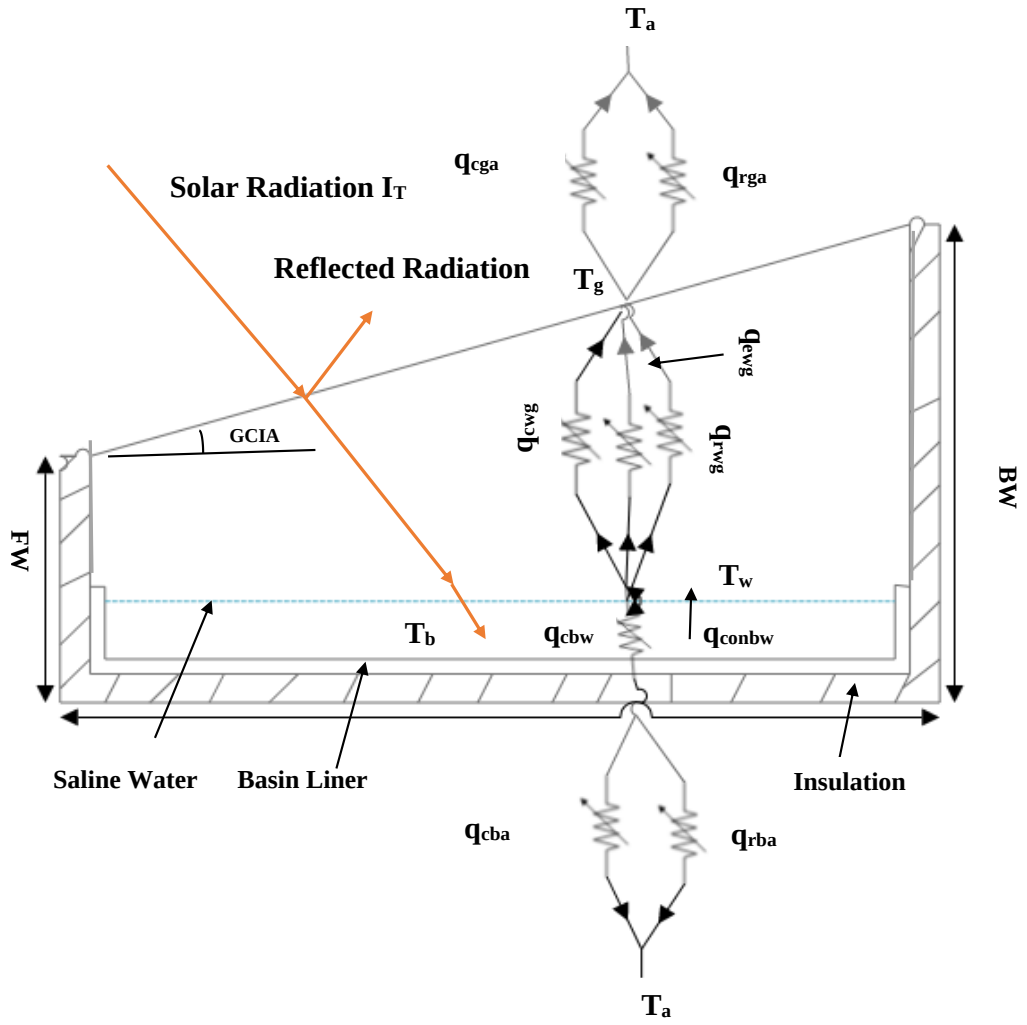

Figure 3.2 Illustrative diagram of the proposed Solar Desalination Still. (Source: Author)

The energy balances at the three boundaries are illustrated by Figure 3.3 (a), (b) and (c) for the glass, water and basin boundaries, respectively.

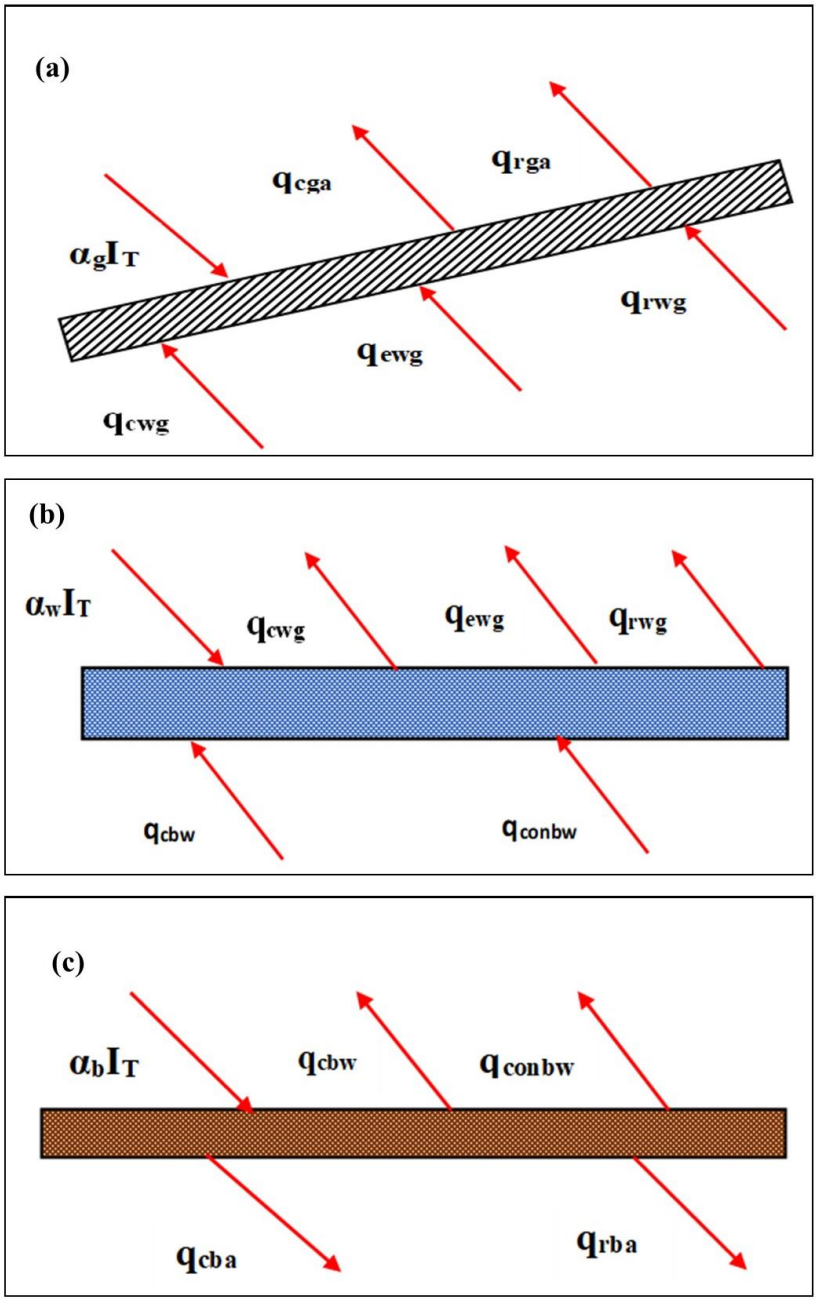

Figure 3.3 Energy balances at, (a) transparent cover, (b) salty water and (c) basin liner (Source: Author)

The corresponding energy equilibrium equations are represented by equations (4), (5) and (6) for the glass cover, water and basin liner boundaries, respectively. (Karimi Estahbanati et al., 2016), (Nian et al., 2021), (Feilizadeh et al., 2017).

$$\frac{dT_g}{dt} = \frac{1}{M_g C_g}((\alpha_g A_g I_T + A_w h_{ewg}(T_w - T_g) + A_w h_{C\omega g}\,(T_w - T_g) + A_w\, h_{r\omega g}(T_w - T_g) - A_g\, h_{cga}(T_g - T_a) - A_g\, h_{rga}(T_g - T_a)) \quad (4)$$

$$\frac{dT_w}{dt} = \frac{1}{M_w C_w}(\tau_g \alpha_w A_w I_T + A_b h_{Cbw}\,(T_b - T_w) + kA_b\,\frac{(T_b - T_w)}{d} - A_w h_{ewg}(T_w - T_g) - A_w h_{C\omega g}\,(T_w - T_g) - A_w\, h_{r\omega g}(T_w - T_g)) \quad (5)$$

$$\frac{dT_b}{dt} = \frac{1}{M_b C_b}\left(\tau_g \tau_w \alpha_b A_b I_T - A_b h_{Cbw}\,(T_b - T_w) - kA_b\,\frac{(T_b - T_w)}{d} - A_b h_{Cba}\,(T_b - T_a) - A_b, h_{rba}(T_b - T_a)\right) \quad (6)$$

The evaporative, convective and radiative heat transfers from the water to the glass cover are expressed as, $A_w h_{ewg}\,(T_w\text{-}T_g)$, $A_w h_{cwg}\,(T_w\text{-}T_g)$, and $A_w h_{rwg}\,(T_w\text{-}T_g)$, respectively. The convective and radiative heat transfer from the glass cover to air are respectively given by $A_g h_{cga}\,(T_g\text{-}T_a)$ and $A_g h_{rga}\,(T_g\text{-}T_a)$. The convective and conductive heat transfers from the basin liner to the water are expressed by, $A_b h_{cbw}\,(T_b\text{-}T_w)$ and $kA_b\ \frac{(T_b - T_w)}{d}$, respectively. Thex convective and radiative heat transfers from the basin liner to surrounding air are given by $A_b h_{cba}\,(T_b\text{-}T_a)$ and $A_b h_{rba}\,(T_b\text{-}T_a)$, respectively.

The radiative heat transfer coefficient h_{rwg} and the evaporative heat transfer coefficient h_{ewg} were determined using the relations in equations (7) and (9), respectively (El-Sebaey et al., 2022) E_{eff} being the effective emittance given by equation (8) (Singh & Gautam, 2022). The convective heat transfer coefficient h_{cwg} was determined using equation (10) (Dhivagar et al., 2024). The σ in equation (7) is the Stephan-Boltzmann constant, whose value is 5.67×10^{-8} W/m^2. K^4 (Singh, 2024).

$$h_{r\omega g} = \varepsilon_{eff}.\sigma\,\frac{\left[(T_w + 273)^4 - (T_g + 273)^4\right]}{(T_w - T_g)} \quad (7)$$

$$\varepsilon_{eff} = \left[\frac{1}{\varepsilon_w} + \frac{1}{\varepsilon_g} - 1\right]^{-1} \quad (8)$$

$$h_{ewg} = 1.6273 \times 10^{-3} h_{cwg} \left[\frac{P_w - P_g}{T_w - T_g}\right] \quad (9)$$

$$h_{c\omega g} = 0.884 \left[T_w - T_g + \frac{(P_w - P_g)T_w + 273}{268900 - P_g}\right]^{1/3} \quad (10)$$

The terms P_w and P_g are the partial vapour pressures for the water and glass surfaces given by equations (11) and (12), respectively (Rejeb et al., 2021) .

$$P_w = \exp\left(25.137 - \frac{5144}{T_w + 273.15}\right) \quad (11)$$

$$P_g = \exp\left(25.137 - \frac{5144}{T_g + 273.15}\right) \quad (12)$$

The relation used to determine the freshwater production rate is as expressed in equation (13) (Nian et al., 2021).

$$\frac{dm_{ew}}{dt} = A_w h_{ewg} \frac{(T_w - T_g)}{L_w} \quad (13)$$

m_{ew} being the solar still freshwater production rate given by equation (14) (Nian et al., 2021).

$$m_{ew} = (3600) A_w h_{ewg} \frac{(T_w - T_g)}{L_w} \quad (14)$$

Where L_w is the latent heat of vaporization, $T_{w\,and} T_g$ are the water and glass cover temperatures, respectively, while h_{ewg} denotes the water-transparent cover heat transfer coefficient.

The energy efficiency (η) of solar still is then defined as the ratio of distilled water produced and the solar energy incident on the still expressed by equation (15) (Nian et al., 2021).

$$\eta = \frac{\Sigma m_{ew} L_w}{I_{T\Delta t}} \times 100\% \quad (15)$$

Δt being the time interval (hours).

The equations were integrated in MATLAB-Simulink by translating them into Simulink blocks. The system components were taken as the glass layer, water and basin liner. The Integrator blocks

were used to represent the different ordinary differential equations that solve the values for the temperatures $T_{g,}$ T_w and T_b. The constant block was used to represent the various constants within the model. The Integrator block was used for integrating the various ordinary differential equations, the gain block was used for the various fractions while the summation and product blocks were, respectively, used for the various additions and products within the model. The model was designed to have the various temperatures, mass of the produced freshwater and solar still efficiency as the output parameters, whereby the scope and display blocks were used for the exhibition of the various output parameters.

The developed model was further employed for the parametric study. For each previously defined liner thickness, the width-to-length ratio was varied across the entire width-to-length ratios range. Similarly, for each previously defined width-to-length ratio, the thicknesses were varied across the entire thicknesses range. The model inputs thus varied for each scenario. For this particular experiment, the thermodynamic traits of synthetic graphite were used. For each simulation, the model computed the heat transfer processes to evaluate the thermal performance of the solar still.

3.5.4 Model Assumptions

Several assumptions were made to aid the model development process. It was assumed that there is even distribution of temperature across the glass cover, water and basin surfaces/areas (Dhivagar et al., 2022), (Mohsenzadeh et al., 2022). It was also assumed that there are no vapour leaks from the basin casing and the areas of the basin and saline water were presumed to be equivalent (Nguyen, 2018), (Dhivagar et al., 2022). The other assumption was that there is constant and uniform solar radiation over the solar still's surface. Uniform salinity and physical properties of the brackish water was also assumed, (Mohsenzadeh et al., 2022). In addition, steady state conditions were considered (Abozoor et al., 2022).

3.5.5 Model Validation

The developed mathematical model was solved using MATLAB and its inbuilt Simulink application. To ensure its accuracy, the model was validated against experimental results carried out by Hassan et al. (2022), El-Sebaii et al. (2015) and Feilizadeh et al. (2017). The validation process involved comparing key parameters such as water temperature, freshwater yields and width-to-length ratios under similar conditions as those in the referenced experiments. For each validation scenario, the experimental parameters adopted by the authors, for instance solar

irradiation, ambient temperature, wind speed, and area of the solar still basin were incorporated into the developed model. Some of the key parameters obtained from the various studies are outlined in Table 3.2.

Table 3.2 Key parameters adopted from the Experiments

Property	**(Hassan et al., 2022)**	**(El-Sebaii et al., 2015)**	**(Feilizadeh et al., 2017)**
Maximum Solar radiation	960 W/m^2	955 W/m^2	900 W/m^2
Wind Speed	2 m/s	2 m/s	2.5 m/s
Solar Still Basin Area	0.5 m^2	1 m^2	0.5625 m^2
Glass cover inclination angle	27°	15°	30°
Water Depth	0.01 m	0.04 m	0.02 m
Hourly ambient temperatures from experiments			
Time in Hours	**(Hassan et al., 2022)**	**(El-Sebaii et al., 2015)**	**(Feilizadeh et al., 2017)**
6:00	25.0	20.0	25.0
7:00	28.0	24.0	30.0
8:00	32.0	27.0	31.0
9:00	34.0	29.0	32.0
10:00	36.0	30.0	34.0
11:00	37.5	33.0	36.0
12:00	40.0	32.0	38.0
13:00	39.0	32.0	39.0
14:00	39.0	32.5	38.0
15:00	41.0	32.0	39.0
16:00	41.0	32.0	38.0
17:00	40.0	31.0	37.0
18:00	40.0	30.0	40.0

The model was then used to predict the solar desalination still's behaviour under those conditions and its outputs were analysed in comparison with the experimental results. The Normalization for the freshwater yield outputs was achieved by ensuring the yields were per unit square meters in all scenarios. This was facilitated by the flexibility of MATLAB in adjusting input parameters. The

comparison focused on the consistency between the predicted and observed values. The differences between the model's forecast and the experimental data were analysed to assess the model's accuracy and reliability under varying operational conditions. The validation process was done to test the developed model's validity before doing further solar still investigations. The Coefficient of Determination (R^2) was the chosen statistical method for the correlation between the model's prediction and the experimental values. In this method, a value closer to 1 indicates a better fit. R^2 values were calculated using the expression in equation (16) (Kutner, 2005).

$$R^2 = 1 - \frac{\Sigma_{i=1}^{n} (E_{i-} S_i)^2}{\Sigma_{i=1}^{n} (E_{i-} \overline{E}_i)^2} \quad (16)$$

Where E_i are the experimental values, S_i the simulated values and $\overline{E}_i$ symbolizes the mean of the experimental values.

3.5.6 Study Simulations

The developed model was used to perform the various simulations. The defined basin study input parameters which are the solar still basin dimensions and liner materials properties were varied to determine how their different values affected the output, which comprised of the glass, water and basin temperatures, fresh water yields as well as efficiency. Optimisation of the design parameters was then done to identify the basin dimensions and liner material variation that maximised solar still efficiency performance.

Convergence of iterative solutions was carefully monitored to guarantee numerical stability and thermodynamic consistency. The ordinary differential equations representing the basin liner, saline water, and glass cover were solved simultaneously at each simulation time step. The solver iteratively updated the basin liner, water and glass temperature temperatures until steady-state or quasi-steady-state conditions were reached.

Convergence was considered achieved when the absolute variation between consecutive iterations of the dependent variables fell below 10^{-6} °C. This tolerance value (10^{-6}) was selected as a standard numerical accuracy criterion commonly used in MATLAB-based thermal simulations, where further changes below this limit do not significantly affect physical accuracy but ensure computational efficiency. Additionally, the freshwater production rate which depends on the temperature differences was tracked as a secondary indicator of convergence. The simulation

proceeded to the next time step only when the temperature stabilized within the defined tolerance range. This approach ensured that the model achieved stable, consistent, and physically meaningful results for all simulated cases.

3.5.7 Data Collection

Data collection was instrumental in understanding the output and optimization of the desalination still. Data was recorded from the various simulation outputs under different input values. This data was used for the analysis. Initial values of solar irradiation, ambient temperature and wind speed are represented by Figure 3.4

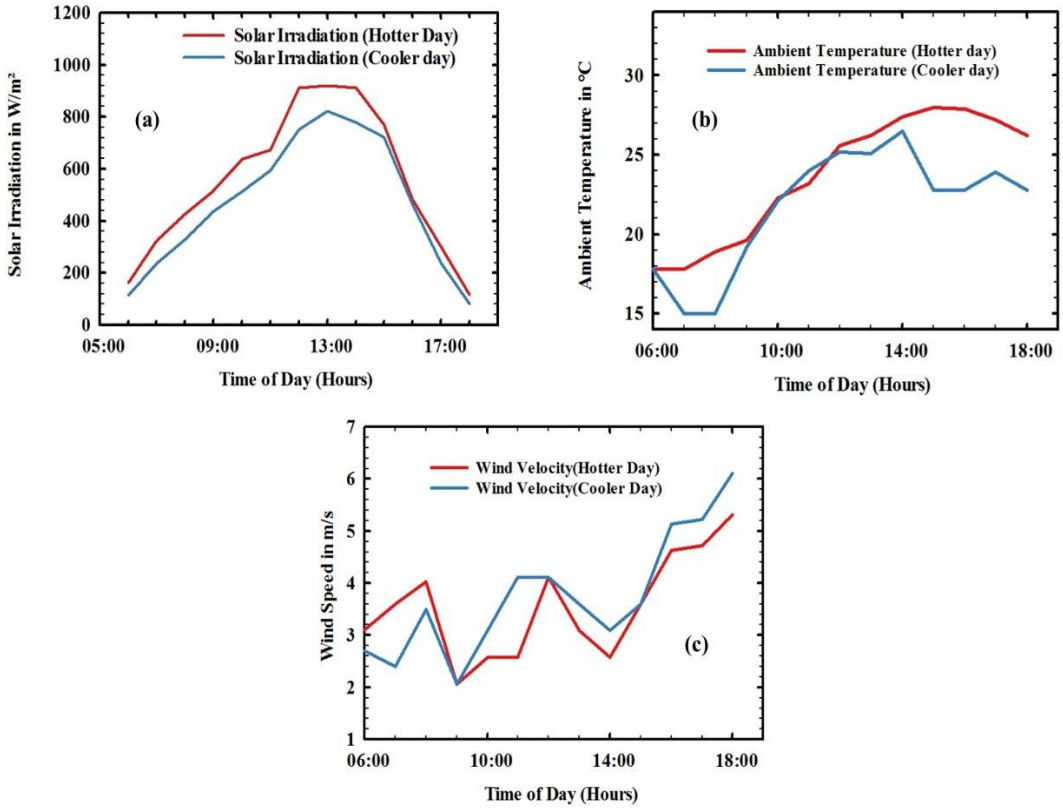

Figure 3.4 Weather data, (a) Solar Irradiation (b) Ambient Temperature and (c) Wind speed (Source: The Kenya Meteorological Department, March 2024)

3.6 Study Materials

The primary tools employed included MATLAB software and Simulink application, which were instrumental in developing and working out the mathematical model of the solar desalination still.

The study therefore relied on computational resources and simulation environments to achieve the research objectives.

Existing research papers and academic articles were studied to provide valuable insights, and they also served as references. Previous course work that was done in year one of postgraduate studies was very instrumental in understanding various heat transfer phenomena. Books and textbooks on solar energy, renewable energy systems and thermal engineering were also very helpful. Online resources helped in staying updated with the latest research developments on solar stills.

3.7 Data Processing and Analysis

Data processing and analysis were critical components of the study as they helped in understanding the implications of the collected data. The recorded simulation outputs were systematically analyzed to dictate the behaviour of the solar still under varying input conditions. This data was further processed to identify the optimal configuration. Part of the processing involved validating the model performance against existing experimental data.

Since this study was conducted through modeling and not physical testing, the quality of the produced water was evaluated using a simple salt-mass balance. During evaporation, only pure water vapor rises and condenses, while the salt remains in the basin brine (Tiwari et al., 1994). To account for possible tiny droplets of salty water that might get carried into the vapor, an entrainment factor was introduced in the model. The amount of salt in the condensed water was then converted into total dissolved solids (TDS) in milligrams per liter this was expressed by equations (17) and (18) (WHO, 2017). If the modeled TDS is below 500 mg/L, the water is considered fresh and safe for drinking as recommended by the (WHO, 2017).

$$\mathrm{m_{salt,d}} = \Sigma f_{\mathrm{e}} C_{\mathrm{brine}}\ \Delta_{\mathrm{md}} \tag{17}$$

Where, f_{e}= entrainment fraction, C_{brine}= salt fraction (kg salt / kg brine), and Δm_d= daily distillate mass

$$TDS = \frac{\mathrm{m_{salt,d}}}{\mathrm{V_d}} \tag{18}$$

$\mathrm{V_d}$ being the distillate volume,

Correlation analysis of parameters such as freshwater yield and variables such as basin dimensions and liner thickness was done. This aided in the parametric analysis which explored the sensitivity of the model efficiency to variations in basin dimensions and liner thickness. This was done by adjusting the values of the input variables within a reasonable range and observing the resulting changes in the efficiency. Findings were presented using visual presentations such as tables, graphs and charts.

CHAPTER FOUR

RESULTS AND DISCUSSIONS

4.1 Introduction

In this chapter, the various results obtained are outlined. Model validation results, the solar still performance under varying basin dimensions, liner material types and thickness are systematically elaborated. Further, parametric study results are outlined thereafter illustrating the interplay between variables.

4.2 Model Validation Results

The developed model was meant to simulate conduction, convection, radiation and evaporation heat transfer processes occurring between the various components of the solar still. Temperature distribution helped understand the heat flux and its impact on freshwater yields. The model enabled variation of input parameters such as materials, thicknesses, masses, areas, densities, emissivities, absorptivities specific heats, dimensions, coefficients of heat transfer, transmissivities, ambient temperatures, wind speeds, solar irradiance and their variation produced varying output parameters such as glass, water, basin temperatures, mass of freshwater yield and solar still efficiency.

From the validation tests, water temperatures in the current model compares favourably with the experiments by (Hassan et al., 2022). It is observed in Figure 4.1(a) that both are in close agreement, with an R^2 value of 0.899 Similarly, the model compares very well with experiments by El-Sebaii et al. (2015), with an R^2 value of 0.993. On the other hand, the cumulative freshwater yields from the current model is in close agreement with experiments by (Hassan et al., 2022) with an R^2 value of 0.984 and as presented in Figure 4.1(b). When compared with experiments by El-Sebaii et al. (2015), the R^2 value is 0.995 with respect to freshwater yields. The study also investigated effects of width-to-length ratios on the yields. The current model obtained optimum freshwater yields at a width-to-length ratio of 0.45 while the experiment by Feilizadeh et al. (2017) produced an optimum yield at a width-to-length ratio of 0.4 as presented in Figure 4.1 (c), implying a close agreement. This then gave an indication of the soundness of the model setting the pace for further study.

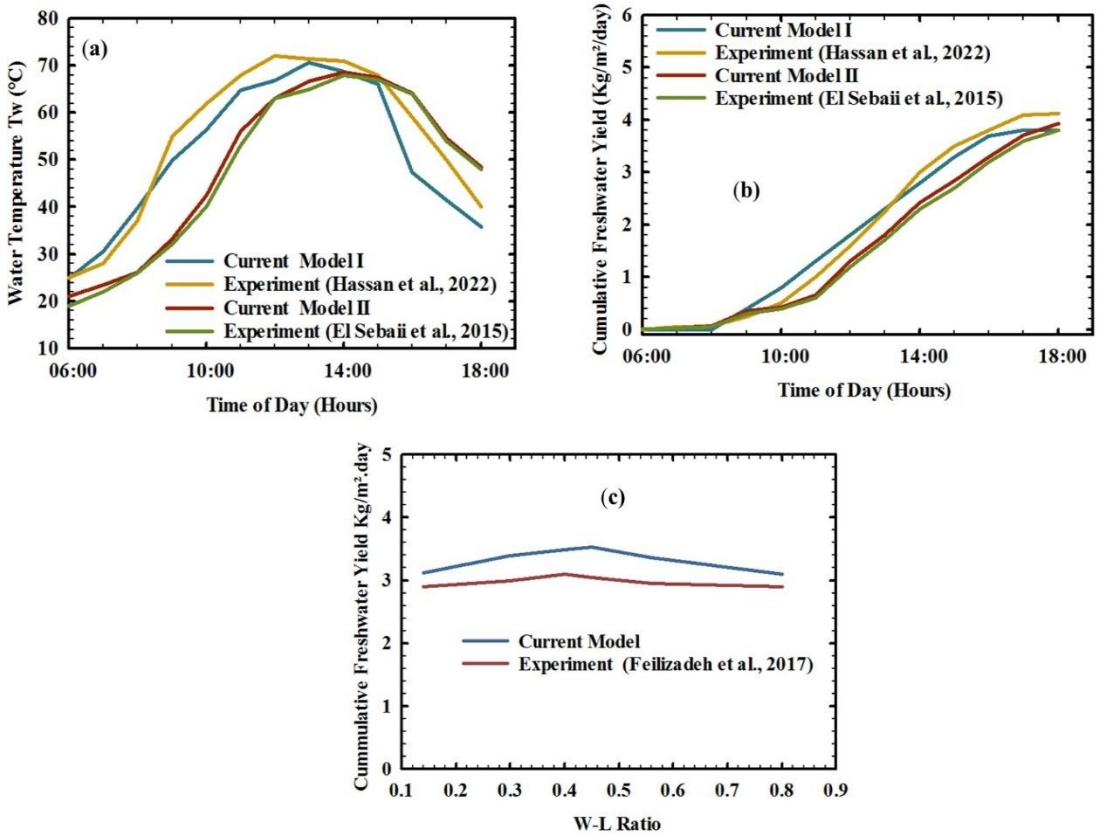

Figure 4.1 Model validation with other studies. (a) Water temperature trends, (b) Cumulative yield trends and (c) Effect of width-length ratio on freshwater yields.

4.3 Freshwater Yields Under Different Basin Dimensions

The effect of basin dimensions was the first item to be investigated. Thermal characteristics of synthetic graphite liner material were utilised for this analysis. The performance of the previously defined width-to-length ratios of 0.14, 0.3, 0.45, 0.56 and 0.8 were investigated. Figure 4.2 outlines the results of the various ratios.

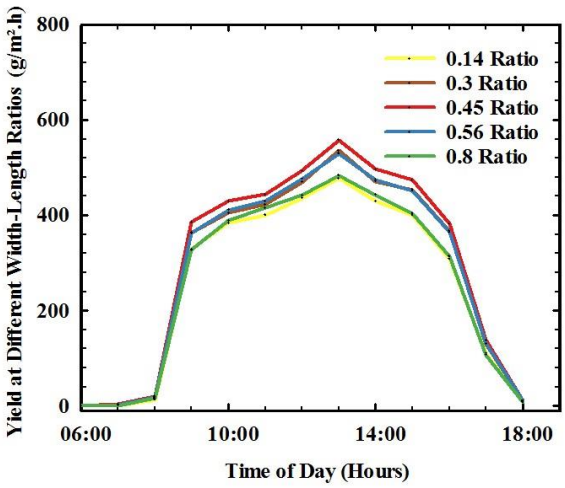

Figure 4.2 Freshwater yield for various width-to-length ratios.

According to Figure 4.2, it is observed that a width-to-length ratio of 0.45 produced the best freshwater yields among the various ratios. With a 0.45 width-to-length ratio, the solar still had the length longer that the width and equal to 1 m and 0.45 m, making it rectangular in shape. A rectangular basin could have the sidewalls shadow effect minimized hence better solar radiation exposure as stipulated by Feilizadeh et al. (2017). Furthermore, the latitude of a location could influence the width-to-length ratio impact as the levels of solar radiations levels vary with latitude, affecting the efficiency of solar energy capture (Duffie & Beckman, 2013). This means that the same width-to-length ratio might perform differently at different latitudes due to the varying solar still tilt angle and the sun-path throughout the year which may affect the overall acceptance angle on the still. Therefore, future solar stills at latitudes near the equator can be implemented using the 0.45 width-to-length ratio regardless of the size of the still for better efficiencies. Subsequent investigations of the study hence maintained a width-to-length ratio of 0.45.

4.4 Solar Still Performance Under Varying Basin Liner Material Types and Thickness.

4.4.1 Solar Still Performance Under Different Basin Liner Material Types

Using 0.45 as the width-to-length ratio, the performance of the different selected basin liner materials was evaluated. The respective volumes and masses for the materials were derived from their densities, thicknesses and still dimensions. The convective heat transfer coefficients between the basin liner and the saline water, the convective heat loss coefficients between the basin liners and the ambient air and the radiative heat loss coefficients between the basin liner and the ambient air were analysed for all the materials and respectively denoted in Figure 4.3.

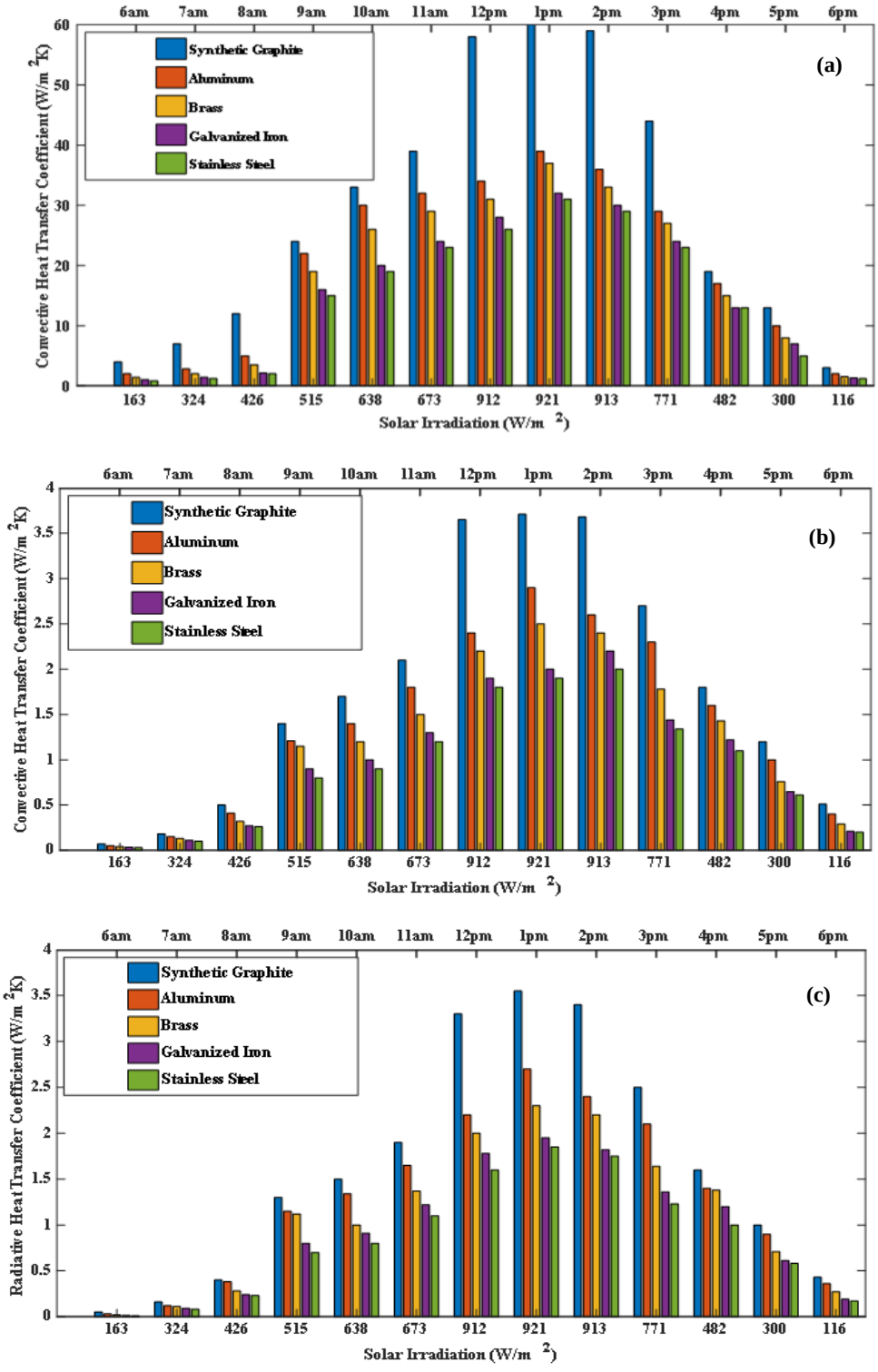

Figure 4.3 Materials heat transfer coefficients at varying irradiation and time of day. (a) Convective heat transfer coefficients between material liners and saline water, (b) convective heat loss coefficients between material liners and ambient air, and (c) radiative heat loss coefficients between material liners and ambient air.

From the Figure 4.3, it is observed that the heat transfer coefficients for all the materials increased with solar irradiation. This coincided with the findings by (Singh et al., 2020) that freshwater production increases with escalating solar irradiation. This coincided with increased temperature differences as a result of the increased basin liner solar absorption. Further analysis of Figure 4.3 shows that the heat transferred from the basin liner material to the saline water is much more than the heat lost from the liner material to the surrounding air. This disparity is evident from the heat transfer coefficient values variations. The immediate contact between the liner material and the saline water facilitates efficient heat transfer, whereas the presence of thermal insulation between the liner material and the surrounding air minimizes heat loss. This observation aligns with established principles of heat transfer, where direct contact enhances heat transfer and insulation reduces convective losses (Tiwari & Sahota, 2017).

Based on the obtained thermodynamic parameters, the performance of the selected liner materials for both the selected days were analysed and presented in Figure 4.4. From the figure, it is worthy observing that synthetic graphite had outstanding freshwater yields in all the scenarios compared to the other materials which are commonly used as solar still basin liner materials like Aluminium, Galvanized Iron and Stainless Steel. This could be attributed to its good thermal properties. Looking into the rest of the materials, Aluminium was the second-best performing material followed by Brass, Galvanized Iron and Stainless Steel, respectively. Brass is not a commonly used solar still basin liner material but from the results, it portrays average performance compared to the other materials. Moreover, the results show that Synthetic Graphite, though also not commonly used as a solar still liner material, is a very potent material that can be considered for future solar still projects.

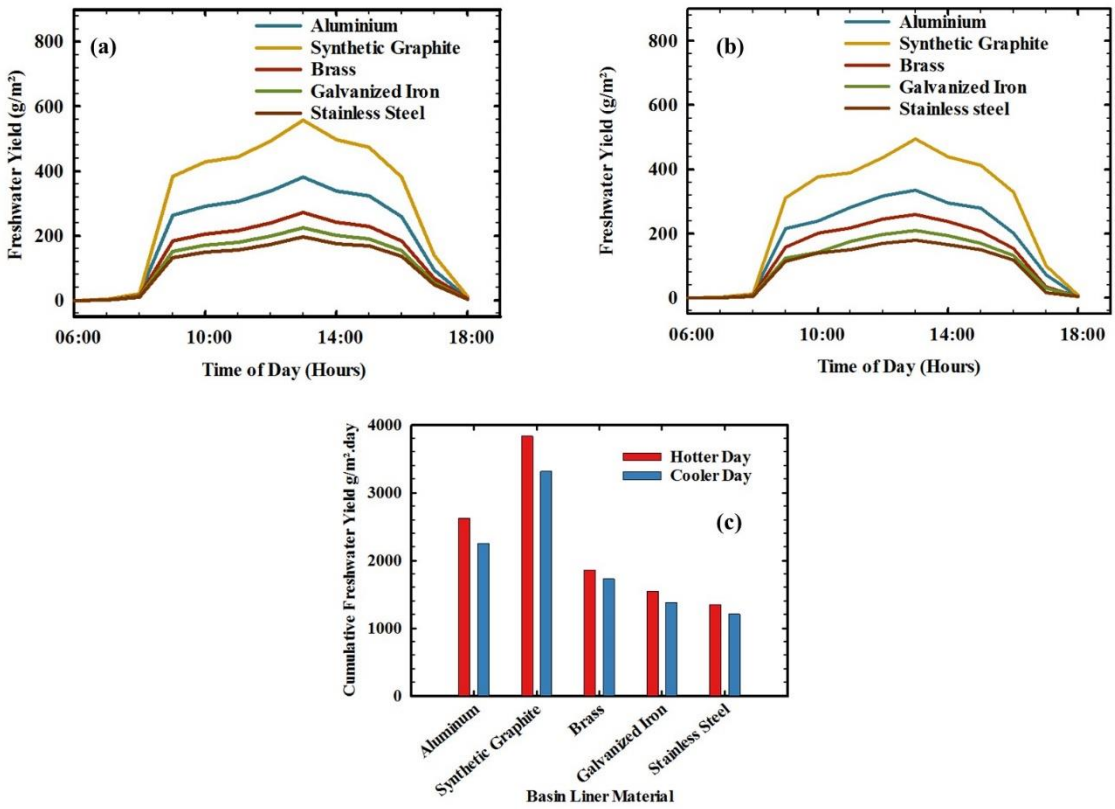

Figure 4.4 Freshwater yields from different liner materials. (a) hotter day, (b) cooler day and (c) yield comparison for the two days.

Further looking into Synthetic Graphite, it demonstrates excellent stability when exposed to harsh weather and saline environments, making it a suitable basin liner material for solar stills. Its non-metallic and crystalline carbon structure provides high resistance to corrosion, oxidation, and chemical attack, even under prolonged contact with saline water (Zhou et al., 2019). Unlike metallic liners, synthetic graphite does not rust or degrade due to chloride ions, and its performance remains consistent under repeated heating and cooling cycles (Han et al., 2020). Additionally, it maintains high solar absorptivity and thermal conductivity, ensuring efficient heat transfer while minimizing maintenance requirements (Yaghoobi et al., 2021). These properties make synthetic graphite an environmentally safe, durable, and thermally effective material for long-term use in solar desalination systems. From this, it can be deduced that selection of the liner material plays a significant role in the performance of a solar still.

4.4.2 Effects of Basin Liner Thicknesses on Still Performance.

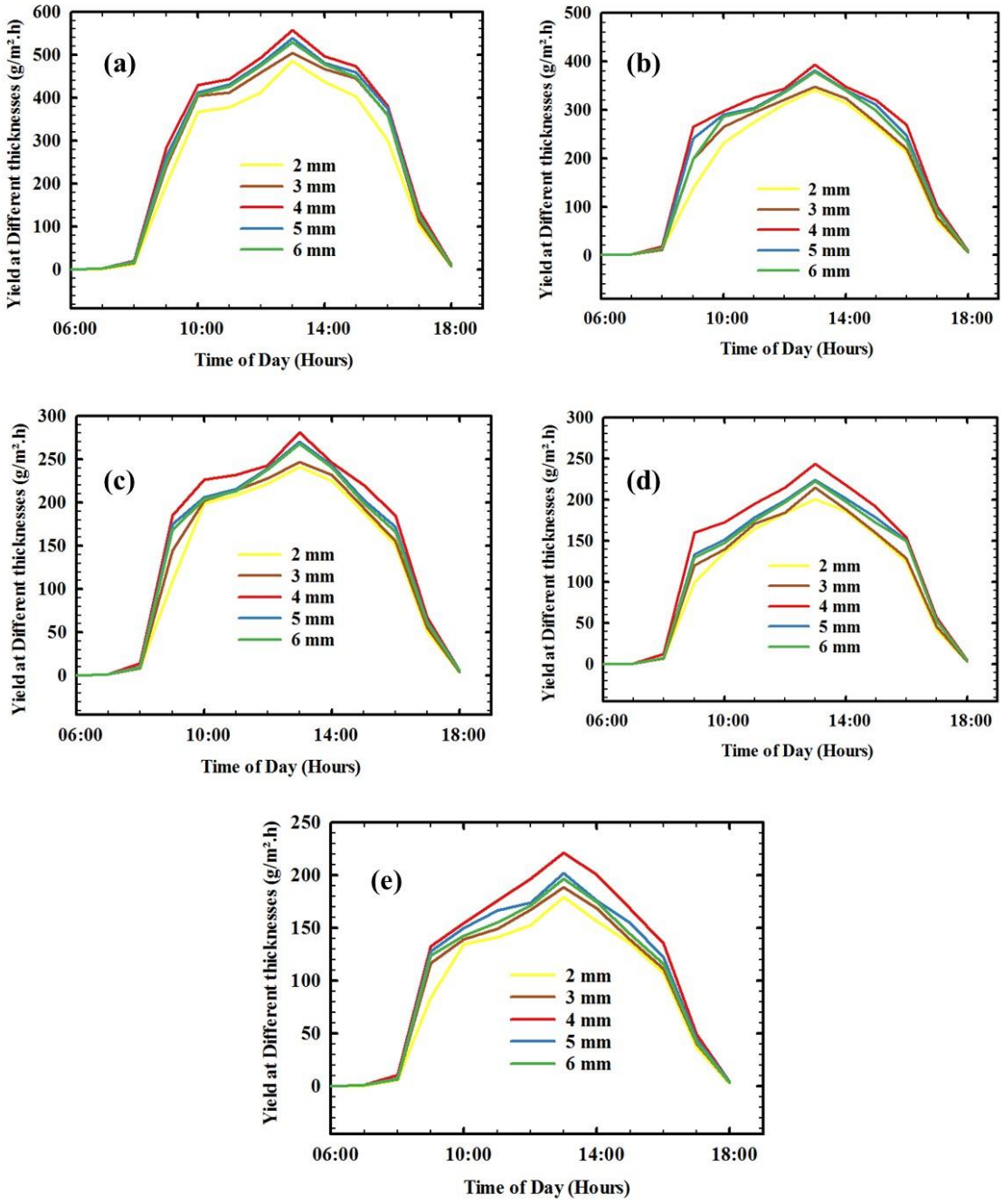

Figure 4.5 Freshwater yields at different liner material thicknesses. (a) Synthetic Graphite (b) Aluminium (c) Brass (d) Galvanized Iron (e) Stainless Steel.

Using the previously established width-to-length ratio of 0.45, the thickness of the five selected liner materials was varied within the model and run in a bid to determine the liner material

thickness with the best freshwater yield. Freshwater outputs were recorded for the various thickness scenarios and the outcomes plotted as shown in Figure 4.5.

Looking at Figure 4.5, it is seen that freshwater yields of the solar still and irrespective of the liner material increased with liner thickness and peaked at 4 mm. Beyond 4 mm, i.e., at 5 mm as well as 6 mm thickness, the productivity of the still decreased which implied that further increase in thickness was not beneficial to the productivity of the solar still. This could be because for thinner liners, (2 mm and 3 mm), the plates have a lower thermal mass leading to faster heating of the liner and the water. However, they equally rapidly lose the thermal energy. Thicker liners (at 5 mm and 6 mm) on the other hand, may take longer times to heat up due to their higher thermal mass. They may also retain the thermal energy for longer as expressed by Lienhard, (2002) and Mugisidi et al. (2018). A thicker liner also increases the thermal resistance and thus decreases the amount of heat transferred by conduction (Iwai et al., 2006).

From this, it can be deduced that striking a balance between the rate of heat absorption and retention is key for a solar still's productivity and development cost. Thinner liners are not very conducive for heat retention while thicker liners may increase the thermal resistance. A 4 mm thickness was thus found to strike the best balance.

4.5 Parametric Study Results Based on Basin Dimensions and Selected Liner Material Thickness

Investigation of the interplay between the basin dimensions (width-to-length ratios in this case) and liner material thicknesses was done via a parametric study. This was to see how those parameters influence each other and their combined impact on the freshwater output of the solar desalination still. This sought to observe how those parameters could be varied or combined in future implementations for improved solar still performance. The thermodynamic traits of synthetic graphite were once again used in this experiment. For each of the scenarios, simulation runs were conducted within the developed model and in each case, the freshwater yield of the still was evaluated. The observed yields were recorded, and the results analysed and then presented as depicted in Figure 4.6.

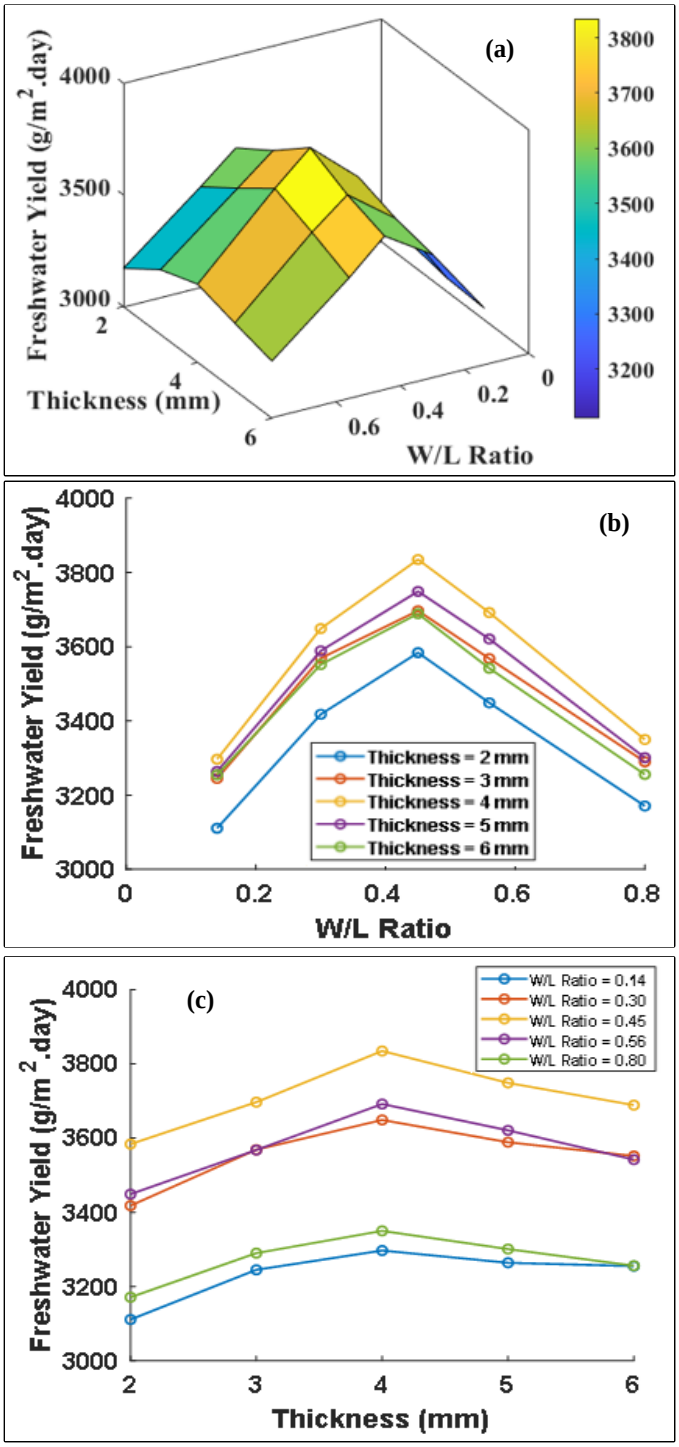

Figure 4.6 Correlation between freshwater yield, width-to-length ratio and liner thickness (a) yields as a function of width-to-length ratio and liner thickness, (b) yields as a function of width-to-length ratio for different thicknesses, and (c) yields as a function of liner thickness for different width-to-length ratios.

From Figure 4.6, the highest freshwater yield is observed at a specific combination of width-to-length ratio (0.45) and liner thickness (4 mm). This indicates an optimal point where the heat transfer characteristics and basin dimensions balance.

The performance of the solar still under the optimal configuration is tabulated in Table 4.1.

Table 4.1 Performance of the solar still at optimal conditions

Time of Day	Tg (°C)	Tw (°C)	Tb (°C)	Freshwater Yield (g./m^2h)	Efficiency (%)
6:00	23.0	24.8	23.4	0.05	0.003
7:00	26.7	32.6	28.5	3.25	0.204
8:00	39.0	41.7	39.8	20.25	1.272
9:00	43.6	49.9	47.4	384.99	24.168
10:00	47.9	54.4	51.7	429.83	26.983
11:00	50.8	63.8	61.7	443.96	27.871
12:00	59.0	66.9	62.4	493.48	30.979
13:00	63.7	70.6	67.2	558.12	35.04
14:00	59.4	68.7	64.1	496.95	31.19
15:00	56.1	66.0	62.3	473.93	29.75
16:00	40.5	47.3	45.5	381.57	23.95
17:00	37.6	41.5	28.3	138.15	8.672
18:00	31.6	35.8	32.4	11.14	0.699

At this optimal point, the solar still's daily yield was 3835 g and the corresponding efficiency was 35.03%. Kaushal & Varun (2010) did a review of efficiencies of various kinds of solar stills designs and operating conditions, and they reported a general range of efficiencies of between 25% and 45%. Based on the optimal yield of 3.835 kg/m²·day obtained for synthetic graphite, the corresponding distillate was evaluated for quality. The total dissolved solids (TDS) of the produced water were found to be approximately 210 mg/L, which is well below the 500 mg/L limit recommended by WHO (2017) for potable water, indicating that the modeled output can be classified as freshwater.

Analysing the current trend, as the width-to-length ratio increases from 0.14 to 0.45, there is a notable increase in freshwater output. Beyond 0.45, the yield starts to decline slightly. This indicates that an excessively elongated basin may not be as effective in capturing and utilizing the incident solar energy. This trend is consistent across all thicknesses, highlighting the significance of basin geometry in optimizing yields. Regarding liner material thickness, it is seen that as the thickness increases from 2 mm to 4 mm, the yields increase too but further increasing the thickness to 5 mm and 6 mm results in a yield decline. This can be attributed to the increased thermal resistance in thicker liners, which impedes efficient heat transfer to the water (Norton, 1992).

Comparing yields across different thicknesses at the same width-to-length ratio, the 4 mm thickness consistently outperformed the other thicknesses, followed by thicknesses of 5 mm, 3 mm, 6 mm, and 2 mm. This suggests that a certain thickness is beneficial for absorbing and retaining heat. This reaffirms the balance between sufficient thermal mass and effective heat transfer.

Quantitative analysis of the impact of these parameters revealed that the width-to-length ratio has a higher significance on freshwater yields compared to liner thickness. Specifically, adjusting the width-to-length ratio from 0.14 to 0.45 resulted in an average increase of 18% in freshwater yield across the thicknesses. Beyond a width-to-length ratio of 0.45, the freshwater yields begin to decline, with an average decrease of 5% as the ratio extends up to 0.8. This suggests that an excessively elongated basin may not be as effective in capturing and utilizing incident solar energy. In contrast, changing the thickness from 2 mm to 4 mm resulted in an average yield increase of 12% across the width-to-length ratios. However, increasing the thickness beyond 4 mm to 6 mm led to an average decrease of 4% in freshwater yields. This can be attributed to the increased thermal resistance in thicker liners as highlighted earlier (Norton, 1992).

Therefore, while both parameters greatly impact the solar still's performance, basin dimensions play a slightly more crucial role than liner thickness in enhancing freshwater yields. Optimizing the width-to-length ratio to 0.45 provides the most substantial improvement, whereas a liner thickness of 4 mm offers the best performance.

In some instances, for example at 3 mm and 6 mm, liners produce approximately the same freshwater yields at a width-to-length ratio of 0.45. With such, one might hence choose a liner material of 3 mm thickness to save on liner material costs for the same solar still output. Hence in designing efficient solar stills, it is crucial to consider both the basin dimensions and liner

thickness. Furthermore, the results indicate that even for materials with excellent thermal characteristics like synthetic graphite, there is an optimal thickness for best performance.

A comparison was made between the current work and some existing studies. The comparison focused on the solar still efficiency as well as the notable differences that could trigger the variation in the efficiency. Table 4.2 shows this comparison.

Table 4.2 Comparison of current work with other studies

Efficiency	Major Differences	Study/Reference
35.04%	Liner Material Synthetic Graphite, width to length ratio 0.45	**Current Study**
19.2%	Liner Material Galvanized steel, width to length ratio 0.53	(Mohsenzadeh et al., 2022)
15.5%	Liner Material Galvanized Irion Sheets, width to length ratio 1	(El-Sebaey et al., 2022)
39.74%	Liner Material Aluminium. width to length ratio 0.49, incorporated flat-plate collectors	(Abozoor et al., 2022)
24.1%	Liner Material Stainless Steel, area 0.5, incorporated snail shells biomaterials	(Dhivagar et al., 2024)

CHAPTER 5

CONCLUSION AND RECOMMENDATIONS

5.1 Conclusion

In this study, impacts of basin dimensions and liner material variance on the performance of a one-slope solar desalination still were investigated. The findings highlighted the significant influence of still geometry and liner material on performance. From the results, synthetic graphite had the best performance, followed by aluminium, brass, galvanized iron and stainless steel with efficiencies of 35.04%, 24.02%, 17.02%, 14.13% and 12.39%, respectively. Thus, synthetic graphite outperformed aluminium, brass, galvanized iron and stainless steel by 31.4%, 51.43%, 59.675 and 64.64%, respectively. It is therefore an excellent liner material choice for solar still fabrication. Further analysis revealed that liner thickness significantly impacts the yield with a 4 mm liner thickness identified as optimal, balancing heat absorption and retention. Additionally, the basin's width-to-length ratio played a crucial role, with a ratio of 0.45 producing the highest freshwater yield. A parametric study examined the interaction between width-to-length ratio and liner thickness. From the study and while liner thickness is important, basin geometry has a greater effect on performance. The results also suggest that thinner liners can achieve comparable yields to thicker ones when the basin geometry is optimized, potentially reducing material costs. These findings offer practical guidance for enhancing solar still performance in future designs.

5.2 Recommendations

From the findings of this work, Synthetic graphite is recommended as a liner material in solar still implementations. The thickness of this liner material should be set at 4mm while the basin width-to-length ratio measurement should be maintained at 0.45 for optimal performance. Further and building on the findings of this research, future studies could explore other innovative materials with better thermal characteristics, durability, and cost. Long-term studies on liner material performance and degradation are essential to ensure sustained efficiency. Research focusing on purifying water possibly by integrating filtration stages or antimicrobial materials may point to new findings.

REFERENCES

Abozoor, M. K. S., Meraj, M., Azhar, M., Khan, M. E., Seraj, M., Ahsan, M., Ahmed, S. A., & Bani Hani, E. H. (2022). Energy and exergy analyses of active solar still integrated with evacuated flat plate collector for New Delhi. *Groundwater for Sustainable Development*, *19*, 100833. https://doi.org/10.1016/j.gsd.2022.100833

Al-Hinai, H., Al-Nassri, M. S., & Jubran, B. A. (2002). Parametric investigation of a double-effect solar still in comparison with a single-effect solar still. *Desalination*, *150*(1), 75–83. https://doi.org/10.1016/S0011-9164(02)00931-1

Al-Maliki, L. A., Al-Mamoori, S. K., Jasim, I. A., El-Tawel, K., Al-Ansari, N., & Comair, F. G. (2022). Perception of climate change effects on water resources: Iraqi undergraduates as a case study. *Arabian Journal of Geosciences*, *15*(6), 503. https://doi.org/10.1007/s12517-022-09695-y

Amir Khadim, M. A. A., Abd AL-Awahid, W. A., & Hachim, D. M. (2020). Review on the types of solar stills. *IOP Conference Series: Materials Science and Engineering*, *928*(2), 022046. https://doi.org/10.1088/1757-899X/928/2/022046

Ayoobi, A., & Ramezanizadeh, M. (2022). A Detailed Review Investigating the Mathematical Modeling of Solar Stills. *Frontiers in Energy Research*, *10*, 879591. https://doi.org/10.3389/fenrg.2022.879591

Bansal, K., Kumar, R., Krishna Mishra, S., Kumar, P., & Sharma, A. (2022). Validation and CFD modeling of solar still with nanoparticle coating on absorber plate. *Materials Today: Proceedings*, *63*, 673–679. https://doi.org/10.1016/j.matpr.2022.04.744

Beng Yeo, K., Meng Ong, C., & Tze Kin Te, K. (2014). Heat Transfer Energy Balance Model of Single Slope Solar Still. *Journal of Applied Sciences*, *14*(23), 3344–3348. https://doi.org/10.3923/jas.2014.3344.3348

Chamsa-ard, W., Fawcett, D., Fung, C. C., Poinern, G., & Murdoch Applied Nanotechnology Research Group, Department of Physics, Energy Studies and Nanotechnology. (2020). Solar Thermal

Energy Stills for Desalination: A Review of Designs, Operational Parameters and Material Advances. *Journal of Energy and Power Technology*, *2*(4). https://doi.org/10.21926/jept.2004018

Cunha, D. P. S., Gomes, V. V., & Pontes, K. V. (2019). Modeling of multi-effect desalination process operated with thermosolar energy applied to the northeastern Brazil. In *Computer Aided Chemical Engineering* (Vol. 46, pp. 1537–1542). Elsevier. https://doi.org/10.1016/B978-0-12-818634-3.50257-5

Dhivagar, R., Mohanraj, M., Hidouri, K., & Belyayev, Ye. (2021). Energy, exergy, economic and enviro-economic (4E) analysis of gravel coarse aggregate sensible heat storage-assisted single-slope solar still. *Journal of Thermal Analysis and Calorimetry*, *145*(2), 475–494. https://doi.org/10.1007/s10973-020-09766-w

Dhivagar, R., Shoeibi, S., Kargarsharifabad, H., Ahmadi, M. H., & Sharifpur, M. (2022). Performance enhancement of a solar still using magnetic powder as an energy storage medium-exergy and environmental analysis. *Energy Science & Engineering*, *10*(8), 3154–3166. https://doi.org/10.1002/ese3.1210

Dhivagar, R., Shoeibi, S., Parsa, S. M., Hoseinzadeh, S., Kargarsharifabad, H., & Khiadani, M. (2023). Performance evaluation of solar still using energy storage biomaterial with porous surface: An experimental study and environmental analysis. *Renewable Energy*, *206*, 879–889. https://doi.org/10.1016/j.renene.2023.02.097

Dhivagar, R., Suraparaju, S. K., Atamurotov, F., Kannan, K. G., Opakhai, S., & Omara, A. A. M. (2024). Performance analysis of snail shell biomaterials in solar still for clean water production: Nature-inspired innovation for sustainability. *Water Science & Technology*, *89*(12), 3325–3343. https://doi.org/10.2166/wst.2024.189

Duffie, J. A., & Beckman, W. A. (2013). *Solar Engineering of Thermal Processes* (1st ed.). Wiley. https://doi.org/10.1002/9781118671603

Dunkle, R., 1961. Solar water distillation: The roof typestill and a multiple effect diffusion stil, in: ASME, Proceeding of International Heat Transfer, Part V, University of Colorado. P. 895. (n.d.).

Ebaid, M. S. Y., & Ammari, H. (2015). Modeling and analysis of unsteady-state thermal performance of a single-slope tilted solar still. *Renewables: Wind, Water, and Solar*, *2*(1), 19. https://doi.org/10.1186/s40807-015-0017-x

Elango, C., Gunasekaran, N., & Sampathkumar, K. (2015). Thermal models of solar still—A comprehensive review. *Renewable and Sustainable Energy Reviews*, *47*, 856–911. https://doi.org/10.1016/j.rser.2015.03.054

El-Sebaey, M. S., Ellman, A., Hegazy, A., & Panchal, H. (2022). Experimental study and mathematical model development for the effect of water depth on water production of a modified basin solar still. *Case Studies in Thermal Engineering*, *33*, 101925. https://doi.org/10.1016/j.csite.2022.101925

El-Sebaii, A. A., & El-Bialy, E. (2015). Advanced designs of solar desalination systems: A review. *Renewable and Sustainable Energy Reviews*, *49*, 1198–1212. https://doi.org/10.1016/j.rser.2015.04.161

El-Sebaii, A. A., Ramadan, M. R. I., Aboul-Enein, S., & El-Naggar, M. (2015). Effect of fin configuration parameters on single basin solar still performance. *Desalination*, *365*, 15–24. https://doi.org/10.1016/j.desal.2015.02.002

FAO. (2020). *Water scarcity in Africa: Challenges and opportunities.* https://www.fao.org/3/cb1447en/CB1447EN.pdf

Feilizadeh, M., Soltanieh, M., Karimi Estahbanati, M. R., Jafarpur, K., & Ashrafmansouri, S.-S. (2017). Optimization of geometrical dimensions of single-slope basin-type solar stills. *Desalination*, *424*, 159–168. https://doi.org/10.1016/j.desal.2017.08.005

Ghanim, F. (2008). *Mathematical modeling of A solar STILL* [Thesis, University of Khartoum]. https://core.ac.uk/download/pdf/71674807.pdf

Hafs, H., Ansari, O., & Bah, A. (2023). Performance evaluation of a production system of solar desalination by using rectangular channels with PCM at different seasons. *Acta Ecologica Sinica*, *43*(4), 690–700. https://doi.org/10.1016/j.chnaes.2022.09.001

Han, S., Qiao, Y., Yan, P., Yan, J., Liu, Y., & Li, L. (2020). Wind turbine power curve modeling based on interval extreme probability density for the integration of renewable energies and electric vehicles. *Renewable Energy*, *157*, 190–203. https://doi.org/10.1016/j.renene.2020.04.097

Hassan, H., Omran Osman, O., & abo-Elfadl, S. (2022). Novel dynamic simulation model and detailed performance evaluation of single slope solar still: Impact of side walls material. *Solar Energy*, *244*, 298–314. https://doi.org/10.1016/j.solener.2022.08.026

Hemmat Esfe, M., Esfandeh, S., Kamyab, M. H., & Toghraie, D. (2021). Simulation of the impact of solar radiation intensity on the performance of economical solar water desalination still in Semnan province. *Case Studies in Thermal Engineering*, *28*, 101471. https://doi.org/10.1016/j.csite.2021.101471

Iwai, H., Tatsumi, K., & Suzuki, K. (2006). Effect of the plate thermal resistance on the heat transfer performance of a corrugated thin plate heat exchanger. *Heat Transfer—Asian Research*, *35*(3), 209–223. https://doi.org/10.1002/htj.20110

Jamil, B., & Akhtar, N. (2017). Effect of specific height on the performance of a single slope solar still: An experimental study. *Desalination*, *414*, 73–88. https://doi.org/10.1016/j.desal.2017.03.036

Kabeel, A. E., Elazab, M. A., El Hadi Attia, M., Elshaarawy, M. K., Hamed, A. K., Alsaadawi, M. M., Elnasr, M. A., & Bady, M. (2024). Exploring the potential of conical solar stills: Design optimization and enhanced performance overview. *Desalination and Water Treatment*, *320*, 100642. https://doi.org/10.1016/j.dwt.2024.100642

Kabeel, A. E., Teamah, M. A., Abdelgaied, M., & Abdel Aziz, G. B. (2017). Modified pyramid solar still with v-corrugated absorber plate and PCM as a thermal storage medium. *Journal of Cleaner Production*, *161*, 881–887. https://doi.org/10.1016/j.jclepro.2017.05.195

Kalbasi, R., Alemrajabi, A. A., & Afrand, M. (2018). Thermal modeling and analysis of single and double effect solar stills: An experimental validation. *Applied Thermal Engineering*, *129*, 1455–1465. https://doi.org/10.1016/j.applthermaleng.2017.10.012

Karimi Estahbanati, M. R., Ahsan, A., Feilizadeh, M., Jafarpur, K., Ashrafmansouri, S.-S., & Feilizadeh, M. (2016). Theoretical and experimental investigation on internal reflectors in a single-slope solar still. *Applied Energy*, *165*, 537–547. https://doi.org/10.1016/j.apenergy.2015.12.047

Kaushal, A. & Varun. (2010). Solar stills: A review. *Renewable and Sustainable Energy Reviews*, *14*(1), 446–453. https://doi.org/10.1016/j.rser.2009.05.011

Kumar, A., & Maurya, A. (2022). Experimental analysis and CFD modelling for pyramidal solar still. *Materials Today: Proceedings*, *62*, 2173–2178. https://doi.org/10.1016/j.matpr.2022.03.360

Kutner, M. H. (Ed.). (2005). *Applied linear statistical models* (5th ed). McGraw-Hill Irwin.

Lienhard, J. H. (2002). *Thermal Energy*. MIT Open Course Ware. https://ocw.mit.edu/courses/16-050-thermal-energy-fall-2002/87d9f4544b7fd64a77201382500d057c_10_part3.pdf

Lisboa, A. A. V., Segurado, R., & Mendes, M. A. A. (2022). Solar still performance for small-scale and low-cost seawater desalination: Model-based analysis and water yield enhancement techniques. *Solar Energy*, *238*, 341–362. https://doi.org/10.1016/j.solener.2022.04.007

Malaeb, L., Aboughali, K., & Ayoub, G. M. (2016). Modeling of a modified solar still system with enhanced productivity. *Solar Energy*, *125*, 360–372. https://doi.org/10.1016/j.solener.2015.12.025

Malik, Y. A.-A. A., & Mohammad, O. A. A. (2023). Experimental investigation of the impact of water depth, inlet water temperature, and fins on the productivity of a Pyramid Solar Still. *Journal of Groundwater Science and Engineering*, *11*(2), 183–190. https://doi.org/10.26599/JGSE.2023.9280016

Mandal, T., Das, J., Rahman, A. T. M. S., & Saha, P. (2021). Rainfall Insight in Bangladesh and India: Climate Change and Environmental Perspective. In Rukhsana, A. Haldar, A. Alam, & L. Satpati (Eds.), *Habitat, Ecology and Ekistics* (pp. 53–74). Springer International Publishing. https://doi.org/10.1007/978-3-030-49115-4_3

Mittal, G. (2021). An unsteady CFD modelling of a single slope solar still. *Materials Today: Proceedings*, *46*, 10991–10995. https://doi.org/10.1016/j.matpr.2021.02.090

Mohsenzadeh, M., Aye, L., & Christopher, P. (2022). Development and validation of a transient model for a passive solar still considering the aspect ratio of the evaporation chamber. *Solar Energy, 244*, 434–447. https://doi.org/10.1016/j.solener.2022.08.059

Mugisidi, D., Heriyani, O., & Fathurahman, H. (2018). Comparison of plastic and stainless-steel as solar still material. *IOP Conference Series: Materials Science and Engineering, 403*, 012089. https://doi.org/10.1088/1757-899X/403/1/012089

Mustafa, I., & Al Ghamdi, A. (2018). Exergy Analysis of Thermal Seawater Desalination—A Case Study. In *Renewable Energy Powered Desalination Handbook* (pp. 491–515). Elsevier. https://doi.org/10.1016/B978-0-12-815244-7.00013-1

Nguyen, B. T. (2018). Factors Affecting the Yield of Solar Distillation Systems and Measures to Improve Productivities. In M. Eyvaz & E. Yüksel (Eds.), *Desalination and Water Treatment*. InTech. https://doi.org/10.5772/intechopen.75593

Nian, Y.-L., Huo, Y.-K., & Cheng, W.-L. (2021). Study on annual performance of the solar still using shape-stabilized phase change materials with economic analysis. *Solar Energy Materials and Solar Cells, 230*, 111263. https://doi.org/10.1016/j.solmat.2021.111263

Norton, B. (1992). *Solar Energy Thermal Technology*. Springer London. https://link.springer.com/chapter/10.1007/978-1-4471-1742-1_6

Omara, Z. M., Kabeel, A. E., & Younes, M. M. (2014). Enhancing the stepped solar still performance using internal and external reflectors. *Energy Conversion and Management, 78*, 876–881. https://doi.org/10.1016/j.enconman.2013.07.092

Panchal, H., & Awasthi, A. (2017). Theoretical modeling and experimental analysis of solar still integrated with evacuated tubes. *Heat and Mass Transfer, 53*(6), 1943–1955. https://doi.org/10.1007/s00231-016-1953-8

Panchal, H., Mevada, D., & Sathyamurthy, R. (2021). The requirement of various methods to improve distillate output of solar still: A review. *International Journal of Ambient Energy, 42*(5), 597–603. https://doi.org/10.1080/01430750.2018.1542630

Prakash, O., Ahmad, A., Kumar, A., Mozammil Hasnain, S. M., & Kumar, G. (2022). Comprehensive analysis of design software application in solar distillation units. *Materials Science for Energy Technologies*, *5*, 171–180. https://doi.org/10.1016/j.mset.2022.01.005

Qasim, M., Badrelzaman, M., Darwish, N. N., Darwish, N. A., & Hilal, N. (2019). Reverse osmosis desalination: A state-of-the-art review. *Desalination*, *459*, 59–104. https://doi.org/10.1016/j.desal.2019.02.008

Rejeb, O., Yousef, M. S., Ghenai, C., Hassan, H., & Bettayeb, M. (2021). Investigation of a solar still behaviour using response surface methodology. *Case Studies in Thermal Engineering*, *24*, 100816. https://doi.org/10.1016/j.csite.2020.100816

Santos, A., & Hernandez, E. (2017). Experimental evaluation of a single slope solar still. *TECCIENCIA*, *12*(22), 63–71. https://doi.org/10.18180/tecciencia.2017.22.7

SDG 6. (2015). *SDG 6*. https://sdgs.un.org/goals/goal6

Singh, A. K. (2023). Mathematical analysis of optimized requisites for novel combination of solar distillers. *Journal of Engineering Research*, *11*(4), 515–525. https://doi.org/10.1016/j.jer.2023.100121

Singh, A. K. (2024). Analysis for optimized prerequisites of modified solar stills. *Heliyon*, *10*(3), e25804. https://doi.org/10.1016/j.heliyon.2024.e25804

Singh, A. K., & Gautam, S. (2022). Optimum techno-eco performance requisites for vacuum annulus tube collector–assisted double-slope solar desaltification unit integrated modified parabolic concentrator. *Environmental Science and Pollution Research*, *29*(23), 34379–34405. https://doi.org/10.1007/s11356-021-18426-x

Singh, A. K. & Samsher. (2021). A review study of solar desalting units with evacuated tube collectors. *Journal of Cleaner Production*, *279*, 123542. https://doi.org/10.1016/j.jclepro.2020.123542

Singh, A. K., Yadav, R. K., Mishra, D., Prasad, R., Gupta, L. K., & Kumar, P. (2020). Active solar distillation technology: A wide overview. *Desalination*, *493*, 114652. https://doi.org/10.1016/j.desal.2020.114652

Sivakumar, V., Sundaram, E. G., & Sakthivel, M. (2016). Investigation on the effects of heat capacity on the theoretical analysis of single slope passive solar still. *Desalination and Water Treatment*, *57*(20), 9190–9202. https://doi.org/10.1080/19443994.2015.1026284

Suraparaju, S. K., Peddojula, M. K., Samykano, M., El-Sebaey, M. S., Kadambari, C. V. K., Budala, S. B., Manepalli, T. V. R., Reddy, L., Vardhanapu, S. R., Ajjada, B. R., & Pilli, R. B. (2024). Enhancing the productivity of pyramid solar still utilizing repurposed finishing pads as cost-effective porous material. *Desalination and Water Treatment*, *320*, 100733. https://doi.org/10.1016/j.dwt.2024.100733

Thakur, A. K., Sathyamurthy, R., Saidur, R., Velraj, R., Lynch, I., & Aslfattahi, N. (2022). Exploring the potential of MXene-based advanced solar-absorber in improving the performance and efficiency of a solar-desalination unit for brackish water purification. *Desalination*, *526*, 115521. https://doi.org/10.1016/j.desal.2021.115521

The National Water Resources Strategy. (2021). *The National Water Resources Strategy*. https://faolex.fao.org/docs/pdf/ken214249.pdf

Tiwari, G. N., & Ahmad, M. J. (2009). Optimization of Tilt Angle for Solar Collector to Receive Maximum Radiation. *The Open Renewable Energy Journal*, *2*(1), 19–24. https://doi.org/10.2174/1876387100902010019

Tiwari, G. N., & Sahota, L. (2017). *Advanced Solar-Distillation Systems*. Springer Singapore. https://doi.org/10.1007/978-981-10-4672-8

Tiwari, G. N., Yadav, Y. P., Eames, P. C., & Norton, B. (1994). Solar distillation systems: The state-of-the-art in design development and performance analysis. *Renewable Energy*, *5*(1–4), 509–516. https://doi.org/10.1016/0960-1481(94)90425-1

United Nations Report. (2021). *The United Nations World Water Development Report 2021 Valuing Water*. United Nations. https://www.unicef.org/wash/water-scarcity

United Nations Water. (2021). *Summary Progress Update 2021: SDG 6—Water and sanitation for all.* https://www.unwater.org/sites/default/files/app/uploads/2021/12/SDG-6-Summary-Progress-Update-2021_Version-July-2021a.pdf

USGS Report. (2018). *USGS Report*. https://www.usgs.gov/special-topics/water-science-school/science/where-earths-water

USGS Report. (2021). *USGS Report*. https://www.usgs.gov/faqs/how-much-earths-water-stored-glaciers

Voutchkov, N. (2017). *Pretreatment for reverse osmosis desalination*. Elsevier.

WHO. (2017). *Guidelines for drinking-water quality (4th ed.).* https://www.who.int/publications/i/item/9789241549950

World Bank. (2020). *Poverty and Shared Prosperity 2020: Reversals of Fortune*. Washington, DC: World Bank. https://doi.org/10.1596/978-1-4648-1602-4

World Bank. (2021). *World Bank Group Gender Strategy Mid-Term Review*. World Bank, Washington, DC. https://doi.org/10.1596/35219

Yaghoobi, F., Jamaati, R., & Jamshidi Aval, H. (2021). Simultaneous enhancement of strength and ductility in ferrite-martensite steel via increasing the martensite fraction. *Materials Chemistry and Physics*, *259*, 124204. https://doi.org/10.1016/j.matchemphys.2020.124204

Zhou, Z., Gao, T., McCarthy, S., Kozbial, A., Tan, S., Pekker, D., Li, L., & Leu, P. W. (2019). Parahydrophobicity and stick-slip wetting dynamics of vertically aligned carbon nanotube forests. *Carbon*, *152*, 474–481. https://doi.org/10.1016/j.carbon.2019.06.012

APPENDICES

APPENDIX I: MATLAB MODEL SCRIPTS

Mass Water Efficiency.h file

```
#ifndef RTW_HEADER_UniqueMassWaterModel_h_
#define RTW_HEADER_UniqueMassWaterModel_h_

#include "rtwtypes.h"
#include "solver_types.h"
#include <cmath>  // For fabs and pow

// State derivatives (continuous-time dynamics)
struct StateDerivatives {
    real_T TempIntegrator1; // Basin liner temperature rate (°C/s)
    real_T WaterIntegrator; // Water mass rate (kg/s)
    real_T TempIntegrator2; // Glass cover temperature rate (°C/s)
};

// State enable/disable flags
struct StateDisabled {
    boolean_T TempIntegrator1; // Basin liner integrator disabled
    boolean_T WaterIntegrator; // Water mass integrator disabled
    boolean_T TempIntegrator2; // Glass cover integrator disabled
};

// Real-Time Model Structure
struct RealTimeModel {
    const char_T* errorStatus;             // Error status string
    RTWSolverInfo solverData;             // Solver information
    StateDerivatives* derivatives;        // State derivatives pointer
    StateDisabled* stateDisabledFlags;    // State enable/disable pointer
```

```
    real_T* continuousStates;             // Continuous states pointer
    int_T* periodicStateIndices;          // Periodic state indices
    real_T* periodicStateRanges;          // Periodic state ranges

    // Solver integration buffers
    real_T odeState[3];                   // ODE state buffer
    real_T odeDerivatives[3][3];          // ODE intermediate derivatives
    ODE3_IntgData integratorData;         // Runge-Kutta ODE3 integration data

    // Model size attributes
    struct {
        int_T numContStates;              // Number of continuous states
        int_T numPeriodicStates;          // Number of periodic states
        int_T numSampleTimes;             // Number of sample times
    } Sizes;

    // Model timing attributes
    struct {
        uint16_T stepCounter0;            // Step counter for base rate
        time_T timeStep;                  // Simulation time step
        uint16_T stepCounter1;            // Auxiliary timing step counter
        SimTimeStep simulationStepType;   // Simulation step type
        boolean_T stopRequested;          // Stop simulation flag
        time_T* currentTimePtr;           // Current time pointer
        time_T timeArray[2];              // Timing array
    } Timing;
};

// Class Declaration for MassWaterModel
class UniqueMassWaterModel {
public:
```

```
    // Disallow copying and assignment
    UniqueMassWaterModel(const UniqueMassWaterModel&) = delete;
    UniqueMassWaterModel& operator=(const UniqueMassWaterModel&) = delete;

    // Constructor and Destructor
    UniqueMassWaterModel();
    ~UniqueMassWaterModel();

    // Model initialization and simulation steps
    void initializeModel();               // Model initialization
    void performStep();                   // Perform one simulation step

    // Accessor for Real-Time Model
    RealTimeModel* getModelData();

    // --- Convergence and Quality Assessment Methods ---
    bool checkConvergence(real_T currentVal, real_T prevVal, real_T tol = 1e-6);
    void computeWaterQuality(real_T initialTDS, real_T producedMass);

    // Getters for reporting results
    real_T getTDS() const { return currentTDS_; }
    real_T getSaltRejection() const { return saltRejection_; }

private:
    // Private member variables
    StateDerivatives stateDerivatives_;   // State derivatives
    StateDisabled stateDisabledFlags_;    // State disabled flags
    RealTimeModel realTimeModel_;         // Real-time model data

    // --- Variables for convergence and TDS monitoring ---
    real_T previousTemp_;                 // Previous water temperature
```

```
    real_T previousMass_;                // Previous freshwater mass
    real_T currentTDS_;                  // Current TDS (mg/L)
    real_T saltRejection_;               // Salt rejection percentage

    // Private helper methods
    void updateContinuousStates(RTWSolverInfo* solverInfo); // Continuous state
update
    void computeDerivatives();                              // Derivative computation
};

#endif // RTW_HEADER_UniqueMassWaterModel_h_

// File Trailer for Modified Code
// [EOF]
```

Mass Water Efficiency.cpp file

```
//
// File: WaterProductionEfficiency.cpp
//
// Code generated for the simulation model 'WaterProductionEfficiency'.
//
// Model version                  : 2.0
// Target hardware                : Intel->x86-64 (Windows64)
// Code design goals              :
//    1. Computational efficiency
//    2. Memory optimization
// Last modified                  : Nov 23, 2024
//

#include "WaterProductionEfficiency.h"
#include <iostream>
#include <cmath>
```

```
#include <cstring>


// Macros for model execution

#ifndef isMajorTimeStep

#define isMajorTimeStep(model)        (((model)->Timing.simTimeStep) ==
MAJOR_TIME_STEP)

#endif


#ifndef isMinorTimeStep

#define isMinorTimeStep(model)        (((model)->Timing.simTimeStep) ==
MINOR_TIME_STEP)

#endif


#ifndef setTimePointer

#define setTimePointer(model, val)    ((model)->Timing.t = (val))

#endif


// Function prototypes

extern void WaterProductionEfficiency_computeDerivatives();


//

// Function to update continuous states using ODE3 solver

//

void WaterProductionEfficiency::updateContinuousStates(SolverInfo *solverInfo) {

    // Define solver matrices

    static const double solverCoefficientsA[3]{0.5, 0.75, 1.0};

    static const double solverCoefficientsB[3][3]{

        {0.5, 0.0, 0.0},

        {0.0, 0.75, 0.0},

        {2.0 / 9.0, 1.0 / 3.0, 4.0 / 9.0}

    };
```

```
    double currentTime = solverInfo->getTime();
    double nextTime = solverInfo->getStopTime();
    double timeStep = solverInfo->getStepSize();

    double *stateVariables = solverInfo->getStateVariables();
    ODE3Data *solverData = static_cast<ODE3Data *>(solverInfo->getSolverData());
    double *savedState = solverData->savedState;
    double *f1 = solverData->derivatives[0];
    double *f2 = solverData->derivatives[1];
    double *f3 = solverData->derivatives[2];

    double stepSizeTimesB[3];
    int stateCount = 3;

    solverInfo->setSimTimeStep(MINOR_TIME_STEP);

    // Save state variables
    std::memcpy(savedState, stateVariables, static_cast<uint32_t>(stateCount) *
sizeof(double));

    // Compute first derivative
    solverInfo->setDerivatives(f1);
    WaterProductionEfficiency_computeDerivatives();

    // Compute intermediate steps
    stepSizeTimesB[0] = timeStep * solverCoefficientsB[0][0];
    for (int i = 0; i < stateCount; ++i) {
        stateVariables[i] = savedState[i] + (f1[i] * stepSizeTimesB[0]);
    }

    solverInfo->setTime(currentTime + timeStep * solverCoefficientsA[0]);
    solverInfo->setDerivatives(f2);
```

```
    this->simulateStep();
    WaterProductionEfficiency_computeDerivatives();

    stepSizeTimesB[1] = timeStep * solverCoefficientsB[1][1];
    for (int i = 0; i < stateCount; ++i) {
        stateVariables[i] = savedState[i] + (f1[i] * stepSizeTimesB[0] + f2[i] *
stepSizeTimesB[1]);
    }

    solverInfo->setTime(currentTime + timeStep * solverCoefficientsA[1]);
    solverInfo->setDerivatives(f3);
    this->simulateStep();
    WaterProductionEfficiency_computeDerivatives();

    // Compute final state variables
    for (int i = 0; i < 3; ++i) {
        stepSizeTimesB[i] = timeStep * solverCoefficientsB[2][i];
    }

    for (int i = 0; i < stateCount; ++i) {
        stateVariables[i] = savedState[i] + (f1[i] * stepSizeTimesB[0] +
                                             f2[i] * stepSizeTimesB[1] +
                                             f3[i] * stepSizeTimesB[2]);
    }

    solverInfo->setTime(nextTime);
    solverInfo->setSimTimeStep(MAJOR_TIME_STEP);

    // ---------------------------------------
    // Convergence Check (New Section)
    // ---------------------------------------
    double maxDerivative = 0.0;
```

```
    for (int i = 0; i < stateCount; ++i) {
        double derivativeMagnitude = std::fabs(f3[i]);
        if (derivativeMagnitude > maxDerivative) {
            maxDerivative = derivativeMagnitude;
        }
    }

    // If derivatives are very small, system has reached steady-state
    const double convergenceThreshold = 1e-6;
    if (maxDerivative < convergenceThreshold) {
        std::cout << "[INFO] Numerical convergence achieved at t = "
                  << nextTime << " s" << std::endl;
    }
}

//
// Simulation step function
//
void WaterProductionEfficiency::simulateStep() {
    if (isMajorTimeStep(this)) {
        solverInfo.setStopTime((timingInfo.currentTick + 1) * timingInfo.stepSize);
    }

    if (isMinorTimeStep(this)) {
        timingInfo.currentTime = solverInfo.getTime();
    }

    // Update the water temperature using derivative equations
    stateData.waterTemperature = stateData.stateVariable1;

    // Update the glass temperature
```

```
    stateData.glassTemperature = stateData.stateVariable2;

    // Calculate temperature gradients
    stateData.tempGradient = stateData.waterTemperature - stateData.glassTemperature;

    // Compute the rate of water mass production
    stateData.waterMassRate = stateConstants.latentHeat * stateData.tempGradient;

    // Calculate overall system efficiency
    stateData.systemEfficiency = (stateConstants.gain * stateData.waterMassRate *
                                  stateConstants.evaporationHeat) /
                                 stateConstants.inputEnergy;

    // Thermal performance equations
    stateData.environmentalLosses = stateConstants.envFactor *
stateData.tempGradient;
}

//
// Initialization function for model parameters
//
void WaterProductionEfficiency::initializeModel() {
    // Initialize state variables and constants
    stateData.waterTemperature = 0.0;
    stateData.glassTemperature = 0.0;

    stateConstants.latentHeat = 2260.0;
    stateConstants.evaporationHeat = 100.0;
    stateConstants.envFactor = 0.85;
    stateConstants.inputEnergy = 920.0;

    std::cout << "[INIT] Model initialized successfully." << std::endl;
```

```
}

//
// Compute TDS (Total Dissolved Solids) and Salinity Removal Efficiency
//
void WaterProductionEfficiency::computeTDS() {
    // Parameters
    double initialTDS = 35000.0;      // mg/L (typical seawater concentration)
    double finalTDS = 210.0;          // mg/L (measured distilled water)
    double whoLimit = 500.0;          // mg/L (WHO permissible limit)
    double producedWaterMass = 3.835; // kg (~3.835 L of distillate)

    // Compute salt removal efficiency
    double removalEfficiency = ((initialTDS - finalTDS) / initialTDS) * 100.0;

    // Compute total salt removed
    double totalSaltRemoved = (initialTDS - finalTDS) * producedWaterMass;

    std::cout << "\n[RESULT] Desalination Performance Summary\n";
    std::cout << "-----------------------------------------------\n";
    std::cout << "Produced Water Mass : " << producedWaterMass << " kg\n";
    std::cout << "Initial TDS         : " << initialTDS << " mg/L\n";
    std::cout << "Final TDS           : " << finalTDS << " mg/L\n";
    std::cout << "WHO Limit           : " << whoLimit << " mg/L\n";
    std::cout << "Salt Removed        : " << totalSaltRemoved << " mg\n";
    std::cout << "Removal Efficiency  : " << removalEfficiency << " %\n";
    std::cout << "-----------------------------------------------\n";

    if (finalTDS <= whoLimit)
        std::cout << "[QUALITY] Water quality meets WHO standards.\n";
    else
```

```
        std::cout << "[WARNING] Water quality exceeds safe limit.\n";
}

//
// Main simulation entry point
//
int main() {
    WaterProductionEfficiency model;
    model.initializeModel();

    // Run one simulation step
    model.simulateStep();

    // Perform TDS calculation after simulation
    model.computeTDS();

    std::cout << "\n[END] Simulation complete.\n";
    return 0;
}
```

APPENDIX 2: APPROVAL LETTER FROM GRADUATE SCHOOL

KENYATTA UNIVERSITY
OFFICE OF THE EXECUTIVE DEAN GRADUATE SCHOOL

E-mail: dean-graduate@ku.ac.ke
Website: www.ku.ac.ke

P.O. Box 43844, 00100
NAIROBI, KENYA
Tel. 020-8704150

Internal Memo

FROM: Executive Dean, Graduate School **DATE:** 14th November 2023

TO: Ms. Ruth Njoki Njuguna **REF:** J104/CTY/PT/39097/2017
C/O Energy, Gas and Petroleum Engineering Department

SUBJECT: APPROVAL OF RESEARCH PROPOSAL

This is to inform you that Graduate School Board, at its meeting on **8th November 2023** approved your Research Proposal for the M.Sc Degree entitled ***"Solar Still Basin Measurements and Liner Material Variance for Improved Water Desalination Efficiency"***.

You may now proceed with your Data collection, subject to clearance with the Director General, National Commission for Science, Technology & Innovation and Ethics Review Committee, Kenyatta University.

As you embark on your data collection, please note that you will be required to submit to Graduate School completed Supervision Tracking and Progress Report Forms per semester. The Forms are available at the University's Website under Graduate School webpage downloads.

Also, please ensure that you publish article(s) from your thesis before submitting it to Graduate School for examination as per the Commission for University Education and Kenyatta University guidelines.

Thank you.

REUBEN MURIUKI
FOR: EXECUTIVE DEAN, GRADUATE SCHOOL

CC. Chairman, Department of Energy, Gas and Petroleum Engineering

Supervisors:

1. Dr. Francis Njoka
   C/o Department of Energy, Gas and Petroleum Engineering
   Kenyatta University

2. Dr. Joseph Muguthu
   C/o Department of Energy, Gas and Petroleum Engineering
   Kenyatta University

APPENDIX 3: APPROVAL LETTER FROM NACOSTI

REPUBLIC OF KENYA

NATIONAL COMMISSION FOR SCIENCE,TECHNOLOGY & INNOVATION

Ref No: **274734**

Date of Issue: **02/September/2024**

RESEARCH LICENSE

This is to Certify that Ms.. Ruth Njoki Njoki of Kenyatta University, has been licensed to conduct research as per the provision of the Science, Technology and Innovation Act, 2013 (Rev.2014) in Machakos on the topic: SOLAR STILL BASIN MEASUREMENTS AND LINER MATERIAL VARIANCE FOR IMPROVED WATER DESALINATION EFFICIENCY for the period ending : 02/September/2025.

License No: **NACOSTI/P/24/39585**

274734

Applicant Identification Number

Director General
NATIONAL COMMISSION FOR SCIENCE,TECHNOLOGY & INNOVATION

Verification QR Code

NOTE: This is a computer generated License. To verify the authenticity of this document, Scan the QR Code using QR scanner application.

See overleaf for conditions

APPENDIX 4: PUBLICATION ASSOCIATED WITH THIS STUDY

ELSEVIER

Desalination and Water Treatment

Volume 320, October 2024, 100851

Solar still basin measurements and liner material variance for improved water desalination efficiency

Ruth Njoki Njuguna, Francis Njoka, Joseph Muguthu

Show more

https://doi.org/10.1016/j.dwt.2024.100851

Highlights

- A mathematical model is developed to study solar still performance.
- A parametric study is conducted to determine the interplay between parameters.
- Width-to-length ratio significantly impacts still performance.
- Liner material type and thickness is also a key design parameter.
- Width-to-length ratio of 0.45 and a liner thickness of 4mm provides best performance.